

T-4094

THE EFFECT OF CONTACT TUBE  
DETERIORATION ON GMAW  
PROCESS STABILITY

by

Marie A Mornis

ARTHUR LAKES LIBRARY  
COLORADO SCHOOL OF MINES  
GOLDEN, CO 80401

ProQuest Number: 10783748

All rights reserved

INFORMATION TO ALL USERS

The quality of this reproduction is dependent upon the quality of the copy submitted.

In the unlikely event that the author did not send a complete manuscript and there are missing pages, these will be noted. Also, if material had to be removed, a note will indicate the deletion.



ProQuest 10783748

Published by ProQuest LLC (2018). Copyright of the Dissertation is held by the Author.

All rights reserved.

This work is protected against unauthorized copying under Title 17, United States Code  
Microform Edition © ProQuest LLC.

ProQuest LLC.  
789 East Eisenhower Parkway  
P.O. Box 1346  
Ann Arbor, MI 48106 – 1346

A thesis submitted to the Faculty and Board of Trustees of the Colorado School of Mines in partial fulfillment of the requirements for the degree of Master of Science (Applied Mechanics).

Golden, Colorado  
Date Marie A Mornis

Sign: \_\_\_\_\_  
Marie A. Mornis

Approved: John P. H. Steele  
Dr. John P. H. Steele  
Advisor

Golden, Colorado  
Date January 8, 1992

Joan Gosink  
Joan P. Gosink  
Professor and Head,  
Department of Engineering

ABSTRACT

Welding tests were conducted in an attempt to identify a through-the-arc weld sensing parameter which responded to contact tube wear. The arc voltage was found to contain characteristics related to wear. A relationship between contact tube wear and the area under the power spectral density curve (PSDA) of the arc voltage in the 0 to 4 Hz range was identified. The number of low frequency fluctuations in the arc voltage, represented by PSDA, steadily increases due to the erosion of the contact tube by the electrode. PSDA reaches a peak value when the maximum line contact between the electrode and the contact tube is reached. Past the peak PSDA values become erratic.

TABLE OF CONTENTS

ABSTRACT . . . . . iii

LIST OF FIGURES . . . . . vi

LIST OF TABLES . . . . . viii

ACKNOWLEDGEMENTS . . . . . ix

Chapter 1. INTRODUCTION . . . . . 1

    1.1 Gas Metal Arc Welding (GMAW) . . . . . 1

    1.2 Definitions . . . . . 3

    1.3 Contact Tube Wear . . . . . 5

    1.4 Contact Tube Failure . . . . . 6

    1.5 Tube Wear With Constant  
        Voltage Power Source . . . . . 7

    1.6 Tube Wear With  
        Pulsed-Current Power Source . . . . . 8

    1.7 Wear Mechanisms . . . . . 9

    1.8 Weld Quality . . . . . 11

Chapter 2. SCOPE . . . . . 12

Chapter 3. EXPERIMENTAL PROCEDURE . . . . . 13

    3.1 Simulated Wear Tests . . . . . 13

    3.2 Actual Wear Tests . . . . . 15

        3.2.1 Wear Test, Group I . . . . . 15

        3.2.2 Wear Test, Group II . . . . . 17

        3.2.3 Wear Test, Group III . . . . . 17

    3.3 Weave Test . . . . . 18

Chapter 4. RESULTS AND DISCUSSION . . . . . 20

    4.1 Simulated Wear Tests . . . . . 20

        4.1.1 Current Analysis . . . . . 20

        4.1.2 Voltage Analysis . . . . . 22

4.1.3	Droplet Frequency Analysis . . . . .	23
4.1.4	Arc Length Analysis . . . . .	26
4.1.5	Discussion of Simulated Wear Tests . . . . .	27
4.2	Actual Wear Tests . . . . .	28
4.2.1	Wear Test Group I . . . . .	28
4.2.2	Wear Test Group II . . . . .	32
4.2.3	Wear Test Group III . . . . .	34
4.2.4	Sectioned Contact Tubes . . . . .	38
4.2.5	Discussion of Actual Wear Tests . . . . .	39
4.2.6	Buckingham Pi Theorem . . . . .	45
4.3	Weave Test . . . . .	52
Chapter 5.	CONCLUSIONS . . . . .	55
Chapter 6.	SUGGESTIONS FOR FURTHER STUDIES . . . . .	57
. . . . .		
	REFERENCES CITED . . . . .	58
	FURTHER REFERENCES . . . . .	59

## LIST OF FIGURES

<u>Figure</u>		<u>Page</u>
1.2.1	Contact Tube and Electrode . . . . .	3
1.2.2	Electrode Positioning: Work Angle and Travel Angle . . . . .	4
1.8.1	Weld Flaws . . . . .	11
3.1.1	Through-The-Arc Image System . . . . .	14
3.3.1	Weave Test . . . . .	19
4.1.1	Mean Current Versus Bore Size . . . . .	21
4.1.2	SDEV of Current Versus Bore Size . . . . .	21
4.1.3	PSD Current - 0 to 100 Hertz for Varying Bore Diameter . . . . .	22
4.1.4	PSD Voltage - 0 to 50 Hertz for Varying Bore Diameter . . . . .	23
4.1.5	Droplet Frequency Characteristics Versus Bore Size . . . . .	24
4.1.6	Droplet Profile with Enlarging Bore Size . . . . .	25
4.1.7	Range of Visible Electrode Length Versus Bore Size . . . . .	26
4.1.8	SDEV of Droplet Frequency Versus Ratio of Bore/Wire Diameters . . . . .	27
4.2.1	Voltage Signal with Increasing Weld Time . . . . .	29
4.2.2	Mean Square Voltage . . . . .	31
4.2.3	PSDA of Group I & Group II Versus Length of Electrode . . . . .	33

4.2.4	Wear Pattern for GMAW Process with Steel Electrode . . . . .	35
4.2.5	PSDA and R Versus Length of Wire Fed (Tube A2) . . . . .	36
4.2.6	PSDA and R Versus Length of Wire Fed (Tube B1) . . . . .	37
4.2.7	PSDA and R Versus Length of Wire Fed (Tube C1) . . . . .	37
4.2.8	PSDA and R Versus Length of Wire Fed (Tube S4) . . . . .	38
4.2.9	Sectioned Contact Tubes . . . . .	40
4.2.10	Electrode and Tube Wear Configuration . . . . .	41
4.2.11	Configuration Parameters Versus Rm (Dm/Do) . . . . .	43
4.2.12	Buckingham Pi Theorem PI1 Versus PI2 . . . . .	50
4.2.13	Buckingham Pi Theorem PI1 Versus PI3 . . . . .	50
4.2.14	Buckingham Pi Theorem PI1 Versus PI4 . . . . .	51
4.3.1	PSD voltage for Stringer and 1 Hz Weave Bead at Time 0 and 3 Minutes . . . . .	52
4.3.2	Weave Geometry and Voltage Signal . . . . .	53
4.3.3	PSDA Versus Length of Electrode for Stringer & Weave Test . . . . .	54

## LIST OF TABLES

<u>Table</u>		<u>Page</u>
4.2.1	Actual Wear Tests - Group I . . . . .	28
4.2.2	Actual Wear Tests - Group II . . . . .	32
4.2.3	Actual Wear Tests - Group III . . . . .	34
4.2.4	Contact Tube Measurements . . . . .	39
4.2.5	Buckingham Pi Theorem Parameters . . . . .	46
4.2.6	Buckingham Pi Constants . . . . .	49

ACKNOWLEDGEMENTS

My sincerest gratitude is extended to Dr. John P.H. Steele for all his understanding and guidance during my graduate program; Dr. Tom Siewert, for sharing his extensive knowledge and welding expertise; Dr. Stephen Liu and Dr. Chidambar Ganesh, for their helpful and insightful comments; and Dr. Tim Quinn for being a patient and cooperative co-worker.

My appreciation is extended to the National Institute of Standards and Technology (NIST), for financial support as well as use of the computer facilities, welding equipment and materials.

A special thanks to my husband, Steve, and our three children, Marisa, Daniel and Theresa, for their patience and understanding throughout my adventures in graduate school.

## Chapter 1

### INTRODUCTION

#### 1.1 Gas Metal Arc Welding (GMAW)

Gas metal arc welding uses a continuously fed, consumable electrode (drawn wire). The electrode passes through a contact tip tube, is then melted and the metal is deposited on the base metal. Current conducted through the contact tube (usually made of copper) and through the electrode melts the electrode by resistance heating and heating from the arc. The arc between the electrode and the base metal, provides the heat necessary for melting the base metal. The molten electrode is deposited on the heated base metal by the force of the arc.

An externally supplied gas, generally an argon mixture, is used to shield the molten weld metal from the atmosphere. Most molten metals react with oxygen and nitrogen causing entrapped slag, porosity, or embrittlement. In addition to shielding the electrode and the base metal from contamination, the inert and reactive gases form the plasma which stabilizes the arc.

Two types of power sources used in GMAW are constant voltage and pulsed current. A constant voltage power source maintains a relatively fixed voltage during welding. A constant voltage power source operates by the following self-

correcting mechanism; the arc length is determined by adjusting the arc voltage at the power source, and the wire feed rate is preset. Any variation in contact-tube-to-work distance, CTWD, is then compensated by an instantaneous change in the current (AWS Welding Handbook, 1991).

In a pulsed current power source, the arc current is pulsed between a high and low current. The high current melts the electrode into droplets and propels them through the arc onto the base metal. The low current maintains the arc between pulses and preheats the electrode. A pulsed current power source typically requires a feedback control system in the wire feeder to compensate for changes in CTWD.

## 1.2 Definitions

Figure 1.2.1, identifies the following parameters:

- CTWD** Contact-Tube-to-Work distance, the distance from the contact tip to the base metal.
- Ls** Electrode Extension, the point of current transfer from the contact tube to the electrode, assumed to be at the exit of the contact tube.
- La** Arc Length, the distance from the point of wire melt to the weld pool.
- Vt** Total Voltage drop from power source to base metal.
- Va** Arc Voltage is the voltage drop from the tip of the electrode to the base metal.
- Vs** Voltage drop from the point of current transfer to the tip of the electrode, in this figure the point of current transfer is assumed to be at the contact tube tip.

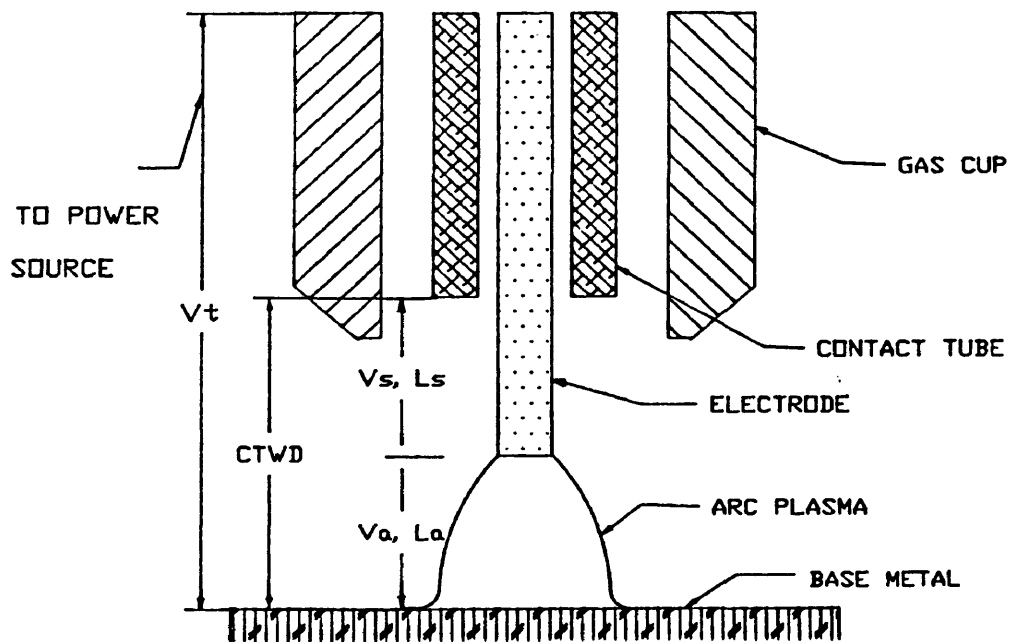


Figure 1.2.1 Contact Tube and Electrode

The electrode orientation can be defined by two angles; the travel angle (leading or trailing) and the work angle, Figure 1.2.2. The travel angle is the angle formed by the axis of the electrode and the plane normal to the direction the welding torch travels. When the tip of the electrode trails the welding gun it creates a stable arc, with little spatter and a narrow bead. Work angle is defined as the angle of the axis of the electrode to the plane normal to the work surface and the work path. Often times the work angle is limited by the accessibility of the weld. For example, fillet welds require a work angle greater than zero degrees in order to deposit the weld bead properly.

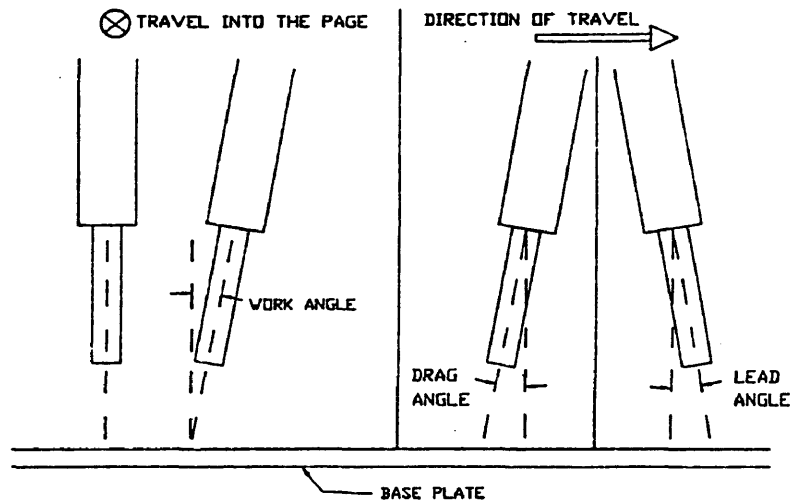


Figure 1.2.2 Electrode Positioning:  
Work Angle and Travel Angle

Travel speed is the rate at which the arc moves across the weld joint. It affects the bead width, penetration, and the amount of heat input to the base metal.

### **1.3 Contact Tube Wear**

A contact tube is usually a copper alloy with bore size 0.2 mm to 0.5 mm larger than the welding electrode, depending on the tube hardness, (DeNale & Lukens, 1986). The tube maintains the electrode position and serves to transfer the welding current from the tube to the electrode.

Maintaining fixed welding parameters such as, CTWD, WFS,  $V_a$  and current, should result in a consistent deposit of weld metal onto the base metal (constant deposition rate). However, when welding with a steel electrode, the contact tube bore size increases due to wear, causing process instabilities. For GMAW of titanium, the tube bore size decreases with weld time and the electrode eventually stops (Denale & Lukens, 1986).

When a contact tube wears during a manual GMAW process, the welder compensates for changes in arc length by moving the welding torch toward or away from the base metal. The welder uses visual and audio feedback as well as years of welding experience to identify a worn tube. As automation of the GMAW process advances a method of automatically monitoring the wear of the contact tube must be developed. An automatic welder

would either compensate for a worn tube or instruct the operator to replace the tube.

#### **1.4 Contact Tube Failure**

Failure of the contact tube can be defined as (1) catastrophic obstruction of the electrode or (2) generation of instabilities in the steady-state welding process. Catastrophic failure interrupts the weld process and replacement of the tube is necessary to continue welding. Instability in the weld process may or may not stop the weld process, but weld quality can deteriorate until the weld will not pass visual acceptance criteria.

There are three types of catastrophic failure of contact tubes; melting the wire to the inside of the contact tube, clogging of the tube due to weld spatter or other debris, and melting the tip of the contact tube. If current consistently transfers to the electrode through a specific region of the tube, the electrode may fuse to the inside of the tube at the current transfer point. This fusion results from the temperature of the system reaching the melting temperature of either the tube, the electrode or both at the current transfer point (Denale & Lukens, 1986). A contact tube tip can also melt from the heat of the arc as the arc length increases. Catastrophic failure happens when debris accumulates inside the tube, causing the wire feed to hesitate and ultimately to

stop.

A contact tube fails to perform properly when instabilities in the steady-state welding process develop. Two examples are; 1. Enlarged contact tube bore diameters created by continuous feeding of the electrode through the tube, causing instability of the current, arc voltage and electrode feed rate. 2. Restricted contact tube bore diameters created by accumulated debris from the electrode or weld spatter, can cause the electrode feed rate to become erratic. The variations in current, arc voltage and electrode feed rate affect weld quality, such as weld profile, penetration, porosity and strength.

### **1.5 Tube Wear with a Constant Voltage Power Source**

In a constant voltage GMAW process, the total voltage ( $V_t$ ) is maintained at a constant setting by the power source. It is assumed that the current transfer point is at the exit of the contact tube, and that electrode extension ( $L_s$ ) is constant during the weld process. However, it is generally assumed that as wear occurs,  $L_s$  may change as the point of current transfer varies (Siewert; 1991). If  $L_s$  increases, current decreases due to an increase in electrode resistance. This results in an increase in voltage drop across the electrode and a decreased voltage drop across the arc ( $V_a$ ). The decrease in  $V_a$ , arc length ( $L_a$ ) and welding current result

in a decrease in power or heat input to the base metal. This reduction in heat may cause insufficient melting of the base metal. With a constant wire feed rate the lower current decreases the electrode melting rate and the electrode may hit the weld pool, causing the arc to short circuit.

#### **1.6 Tube Wear with a Pulsed-Current Power Source**

A GMAW process which uses a pulsed-current power source and a voltage feedback control of the wire feed speed reacts to contact tube wear in the following manner. The current is maintained at a set value by the power source. When the arc length ( $L_a$ ) changes due to wear, it causes a change in arc voltage ( $V_a$ ). Then the feedback control system responds by increasing or decreasing the wire feed speed. Overshoot in the WFS creates oscillation in the arc length until the system stabilizes. If operating with a high travel speed, the variations in arc length affect weld quality by changing the bead width.

Weld quality may also be affected by increased contact tube wear due to changes in the electrode position which may exceed position tolerances. Catastrophic failure of the contact tube can occur when the increase in arc length is so large that the heat of the arc melts the contact tube, stopping the electrode.

### **1.7 Wear Mechanisms**

Wear, in the case of sliding contact between two bodies, is the removal of surface material and severe transformations in surface appearance. Several possible wear mechanisms may be occurring simultaneously in a contact tube during GMAW. This adds to the complexity of identifying specific wear mechanisms, however it appears the combination of abrasion and adhesion contribute to the deterioration of a contact tube.

Abrasive wear is the removal of material by a hard asperity between the contact tube and the wire, or the addition of a foreign body. Foreign bodies may be oxides embedded in the surface or wear particles formed during sliding. Resistance to abrasive wear is a function of hardness and experiments have shown that abrasive wear occurs when the Vickers Hardness (HV) of the asperity is 1.5 times greater than the abraded surface (Schey, 1983). Even if the difference in hardness between the electrode and the contact tube were less, oxides and intermetallics (formed by diffusion when heat is present) may meet this criterion.

A steel electrode (ER 100S) with a tensile strength of 100-110 ksi corresponds to a hardness of 205 HV to 222 HV (Technical Data Handbook, 1984) and the HV of a copper alloy is approximately 70 (ASTM, 1991). Therefore the electrode hardness is 2.92 to 3.20 times greater than the contact tube and abrasion is a viable wear process.

Adhesion wear can be due to cold welding or hot welding. In a GMAW environment the electrode may become contaminated by debris, develop an oxide or be coated with a lubricant to enhance feeding. In spite of this cover, virgin surfaces can be exposed. New surfaces are generated by asperities plowing through surface films of lubricants or oxides. Cold welding between the virgin surfaces of the electrode and the contact tube, creates a junction which can be destroyed by the sliding motion of the electrode. If the junction is as strong or stronger than the contact tube material, the junction separates either at the electrode or at the contact tube. A GMAW process using a steel electrode and a copper alloy contact tube, would indicate junction failure at the tube surface, because the tube diameter increases with weld time.

A GMAW process using a titanium electrode and a copper alloy contact tube, is an example of adhesion wear due to hot welding. With a welding temperature of 1493 K a localized pool of copper develops within the tube. Any titanium added to the molten copper decreases melting temperature until the eutectic point is reached. Any additional titanium added increases the melting point until the pool solidifies resulting in an accumulation of intermetallics inside the contact tube (Denale & Lukens, 1986).

The removal of surface material can be quantified by wear volume. Wear volume (V) is proportional to the distance (l)

or time of sliding.

The following equation reflects this relationship:

$$\frac{V}{L} = \frac{K}{H}$$

where H is the hardness of the softer material and K is some constant specific to the wear conditions. This constant may be a function of the normal load, the area of contact or the shape of the asperity (Schey, 1983).

### 1.8 Weld Quality

Weld integrity can often times be determined by the physical appearance of the weld. Properties such as, dimensional accuracy, amount of distortion, cracks, undercuts, underfills, overlaps, porosity, slag inclusions and joint penetration affect weld quality, Figure 1.8.1.

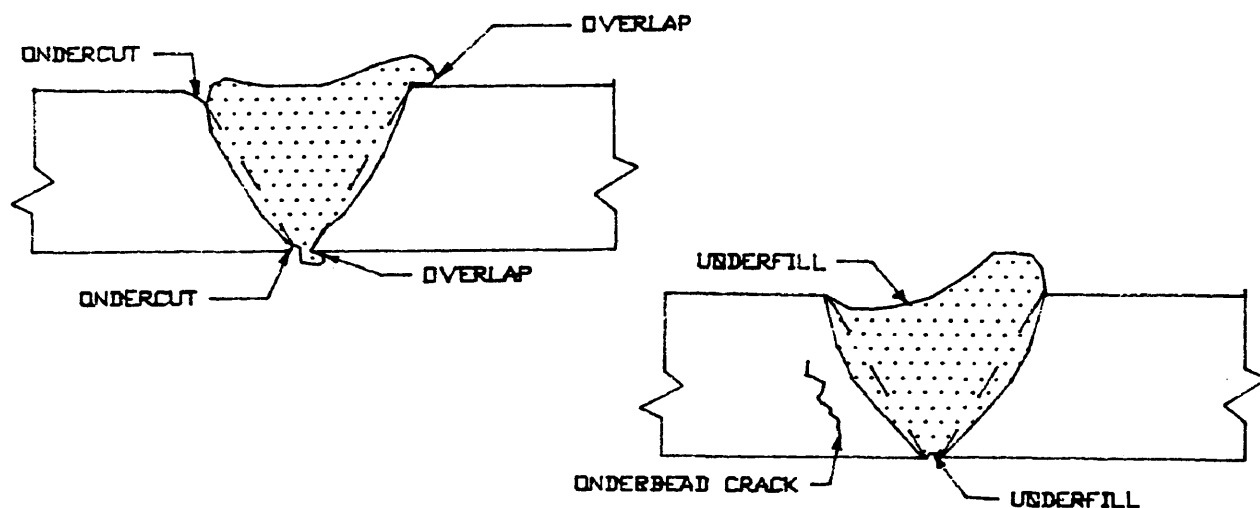


Figure 1.8.1 Weld Flaws

## Chapter 2

### SCOPE

As part of this study, experiments were conducted to discover a through-the-arc sensing parameter which would indicate contact tube wear. The first set of tests attempted to simulate wear by drilling increasing bore diameters for the contact tubes and analyzing the current and droplet frequency data. Plots of mean, standard deviation and power spectral density of the current with changing bore size were developed, along with standard deviation of droplet frequency.

Actual wear tests were conducted ranging from 1 to 8 hours using a pulsed-current power source. The power spectral density of the voltage was analyzed to determine its variation with wear. A comparison of the area under the power spectral density curve of the voltage in the low frequency range (0 to 4 Hz) and change in bore outlet diameter were compared to the total length of electrode consumed during welding. An additional weld test was conducted with a 1Hz weave to determine the effects of the low frequency weave on the power spectral density voltage data.

## Chapter 3

### EXPERIMENTAL PROCEDURE

#### 3.1 Simulated Wear Tests

A test was designed to simulate wear of a contact tube by changing the tube bore diameter. Using a constant voltage power source and constant wire feed rate, the voltage and current were monitored and analyzed. Droplet frequency, the rate of formation of drops of molten electrode which are propelled to the weld pool, was calculated by using a through-the-arc imaging system (Heald, 1990).

A Miller power source [DeltaWeld 650] set at 32 Volts and 300 Amperes, continuously fed the electrode through the tube. The constant potential power source was then filtered by a Kusko DC current regulator. The polarity was direct current electrode positive (DCEP) in which the welding electrode is positive and the base metal is negative.

A Miller [Milleromatic model A-54A] wire feeder set at 10 m/min, in conjunction with a stationary Bug-0 tracking system was used. A stationary, water-cooled, straight welding gun was positioned with the work and travel angles set at zero. The base metal velocity or travelspeed was 20 cm/min (8"/min), the CTWD was 13.5 mm and the shielding gas was a mixture of 95% argon and 5% carbon dioxide.

The through-the-arc imaging system consisted of a helium-neon laser [Spectra-Physics, model #106-1], a high speed video camera [Kodak Extapro 1000], a mirror, two focusing lenses, a narrow band-pass laser filter, and a frosted glass projection screen, Figure 3.1.1.

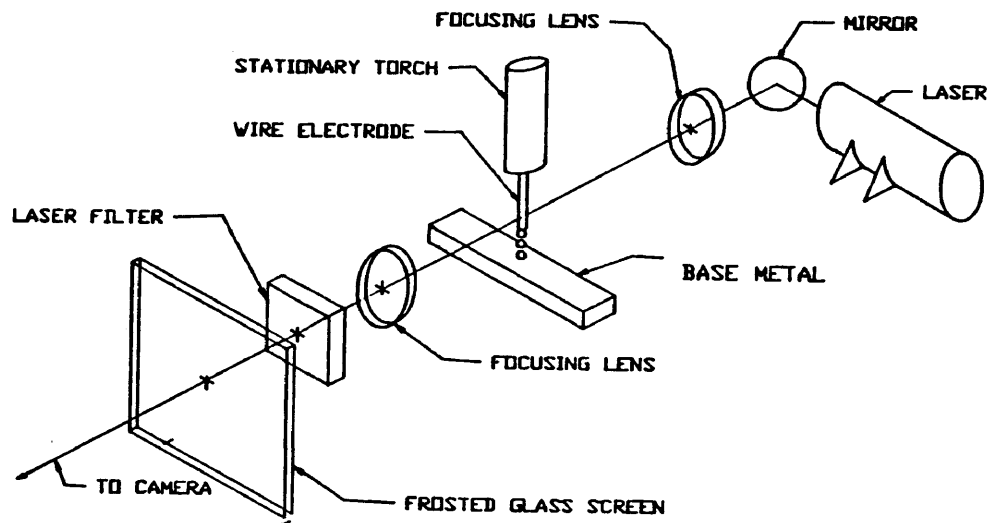


Figure 3.1.1 Through-The-Arc Image System

Standard contact tubes [L-Tec 045H] with a 0.055 in/1.4 mm bore diameter were drilled to 1.5 mm, 1.6 mm, 1.7 mm, 1.8 mm, 1.85 mm, 2.0 mm, 2.1 mm, and 2.24 mm diameters. One contact tube [UCAR 030H] with a 0.050 in/1.3 mm bore diameter was used to represent an undersized bore. The electrode was a stainless steel E70S-3 with a 0.45 in/1.14mm diameter.

Three welds of 8 seconds duration were conducted on each contact tube, for a total of 30 welds. The welding voltage and amperage were acquired using the program ASYST (ASYST, 1988) at an acquisition rate of 2000 samples/sec.

The following data was calculated for each contact tube;

1. Mean and standard deviation of current
2. Power spectral density of current PSD
3. Droplet frequency
4. Length of electrode from the gas cup to the arc

### **3.2 Actual Wear Tests**

3.2.1 Wear Test, Group I. The actual wear tests were conducted in three groups. Group I used a pulsed current power source [Hobart UltraWeld 500] with feedback control of the wire feed speed. The polarity was direct current electrode positive (DCEP). A curved water-cooled weld torch was used with a 0° work angle and a 10° trailing travel angle. The Bug-O tracking system was set at a travel speed of 14.7 cm/min (6

in/min) and the CTWD was 19 mm. Shielding gas was a mixture of 95% argon-5% oxygen at 1.13 m<sup>3</sup>/hr (40 cfh) and contact tubes designed for long life [Tweco 14L-45 1.2 mm] were used. The acquisition rate was 2000 samples/sec and the average current setting ranged from 225 A to 250 A.

The average dimensions of the carbon steel base metal plates were 25 cm x 50 cm x 2 cm (10"x 20"x 3/4"). With the curved torch, welding proceeded along the length of the base metal plate for approximately 3 minutes and after each weld the CTWD was checked and the torch was repositioned. Repositioning was necessary to maintain a consistent direction of travel and corresponding drag angle.

The current and wire feed speed were measured from internal test points provided by Hobart (TP14 for current and TP26 for WFS). The internal WFS test point measures the input voltage to the wire feed motor, and is generated by the internal feedback control system of the UltraWeld 500 power supply. It is not necessarily indicative of the actual wire feed speed. The voltage was measured across the power supply to the base metal. A computer based data acquisition system was used to sample and store large amounts of welding data for later analyses. ASYST, a high level programming language, was used for data acquisition of the voltage and WFS, with acquisition rates of 200, 800 and 2000 samples/s and the low pass filter (to eliminate the aliasing) was set at the Nyquist

frequencies 90 Hz, 360 Hz and 900 Hz, respectively. The power spectral density, PSD, of the voltage was calculated for analysis.

3.2.2 Wear Test, Group II. Group II is similar to Group I except that Tweco tubes model 14-45 1.2 mm were used instead. The mean amperage setting ranged from 150 A to 220 A and the data acquisition rates for voltage and WFS were 200, 220 and 2000 samples/s. For the lower sampling rates the signal was first sent through a 90 Hz and 100 Hz low pass filter [KROHN-HITE CORPORATION Model 3202] before computer acquisition. The power spectral density of the voltage and area under the curve of the PSD of the voltage from 0 to 4 Hertz were calculated from the acquired data.

3.2.3 Wear Test, Group III. Group III used the Hobart UltraWeld 500 pulsed-current power source and a straight water-cooled weld torch with 0° work and travel angles. Hobart tubes models HB177000 .045-54, HB177059 .045-54 and HB379296 .045-52 were used. The straight torch did not require repositioning, however, every 9 to 18 minutes the welding was stopped to check CTWD (19 mm) and measure the change in contact tube diameter with calipers. The shielding gas was 95% argon-5% CO<sub>2</sub>, the mean operating amperage was 300 A, the voltage and WFS data acquisition rate were 200

samples/s and the low pass filter was set at 90 Hz. The following information was calculated from the acquired data;

1. Power spectral density of voltage PSD
2. Area under the curve of the PSD of  $V_a$
3. Wear volume, contact surface and arc length for tube

### **3.3 Weave Test**

A weave of 1 Hz was introduced to the actual wear tests to determine its effect on the low frequency PSD data. The low frequency voltage signal, introduced by changes in the CTWD due to weave geometry, is within the 0 to 4 Hertz frequency range of the power spectral density data. The test utilized the Linde torch set at a  $0^\circ$  work angle and a  $10^\circ$  drag angle, with a Tweco 14-45 1.2 mm tube. The shielding gas mixture was 95% argon-5%  $CO_2$ , the travel speed was set at 14.7 cm/min (6"/min) and the acquisition rate was 220 samples/sec. A 6 mm thick steel bar was tack-welded to the base metal plate and tilted to approximately a  $45^\circ$  angle to simulate a V-groove joint, Figure 3.3.1. The stroke on the horizontal oscillator was set to 10 mm and the CTWD was 19 mm.

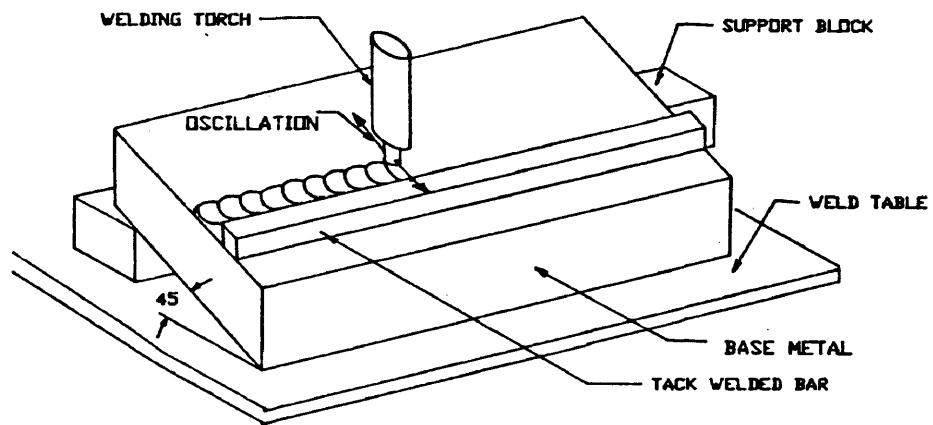


Figure 3.3.1 Weave Test

## Chapter 4

### RESULTS AND DISCUSSION

#### 4.1 Simulated Wear Tests

4.1.1 Current Analysis. The mean and standard deviation of the welding current were calculated and plotted for the three weld tests conducted for each bore size. Figure 4.1.1 is the graph of average mean current versus bore size (1.4 mm is standard bore), and Figure 4.1.2 is the graph of the standard deviation of current taken at each bore size. From previous experiments, (Heald, 1990) a small increase in the standard deviation of the weld current occurred with an increase in bore diameter. However, the results of these tests do not show a definite or consistent increasing trend in standard deviation of current.

The power spectral density (PSD) curve from 0 to 1000 Hertz is calculated using the Fast Fourier Transform method (Bendant and Peirsol, 1971). Figure 4.1.3 shows the PSD current curves for varying bore diameter from 0 to 100 Hertz. This range was selected for analysis because it contained the most diversity in the PSD magnitude. However, no consistent trend in current PSD magnitudes corresponded to increasing bore diameters.

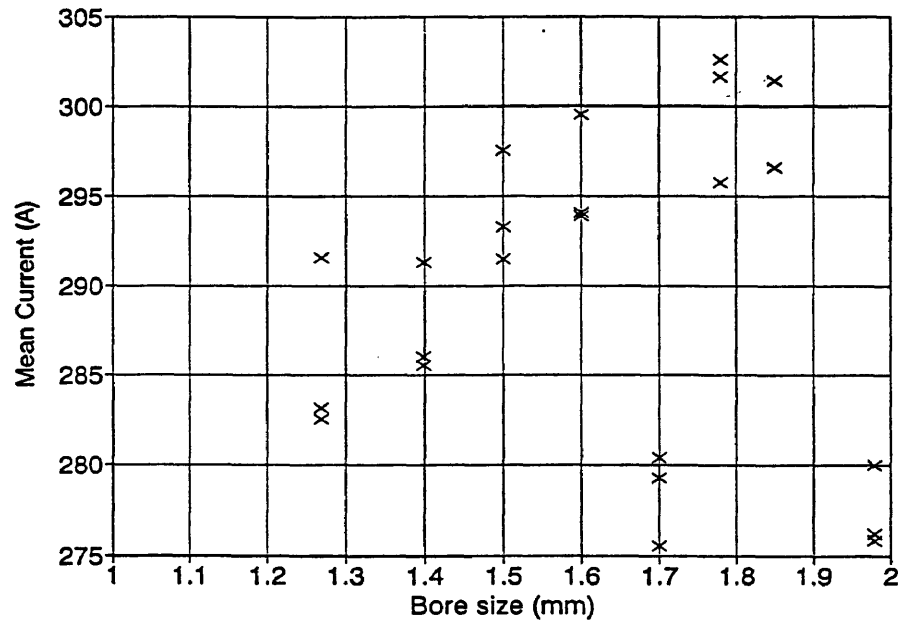


Figure 4.1.1 Mean Current Versus Bore Size

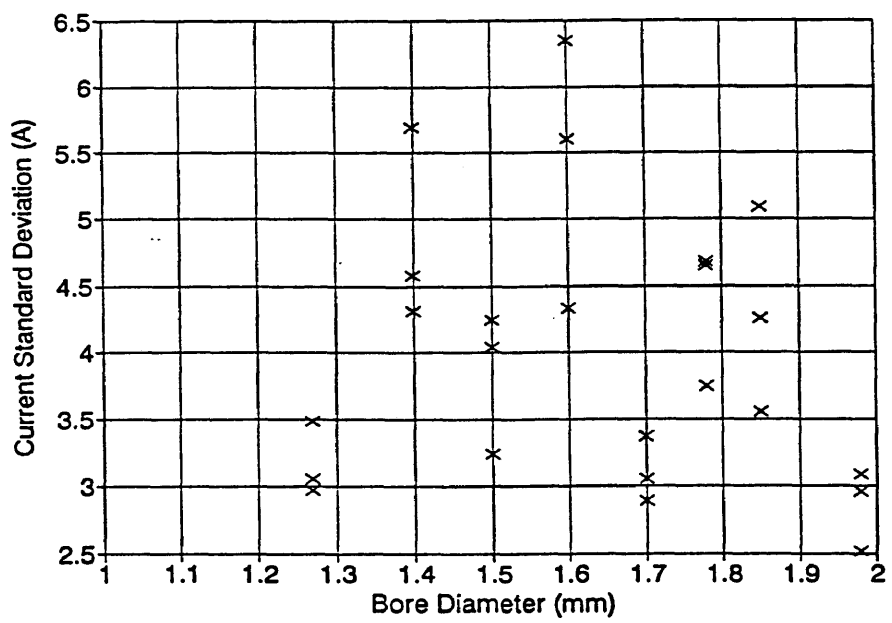


Figure 4.1.2 Current SDV Versus Bore Size

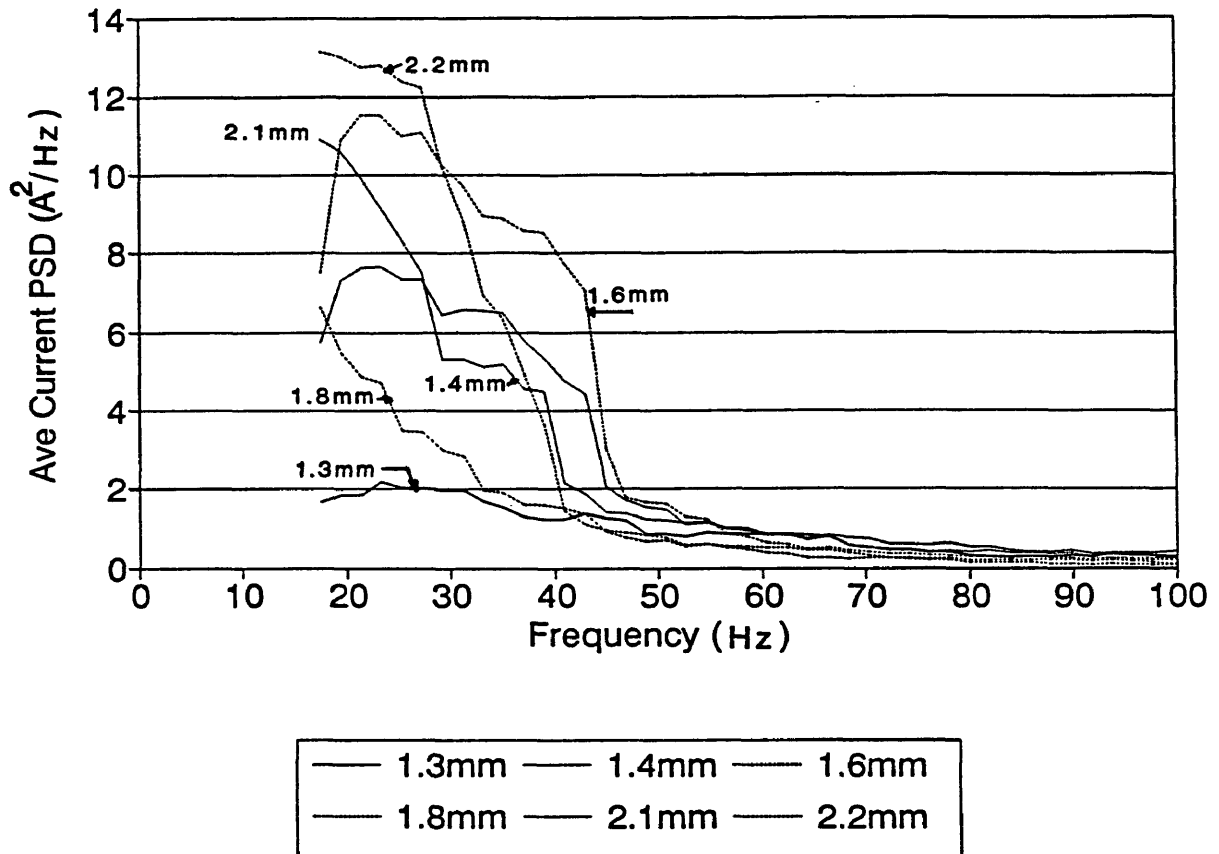


Figure 4.1.3 PSD Current - 0 to 100 Hz for Varying Bore Diameter

4.1.2 Voltage Analysis. One effect of wear in a contact tube is erratic arc length and corresponding arc voltage ( $V_a$ ), therefore the PSD of the arc voltage data was calculated and plotted Figure 4.1.4. The lower frequency range of 0 to 50 Hertz was selected for observation, and does not show a steady increase in magnitude of the voltage PSD with bore diameter.

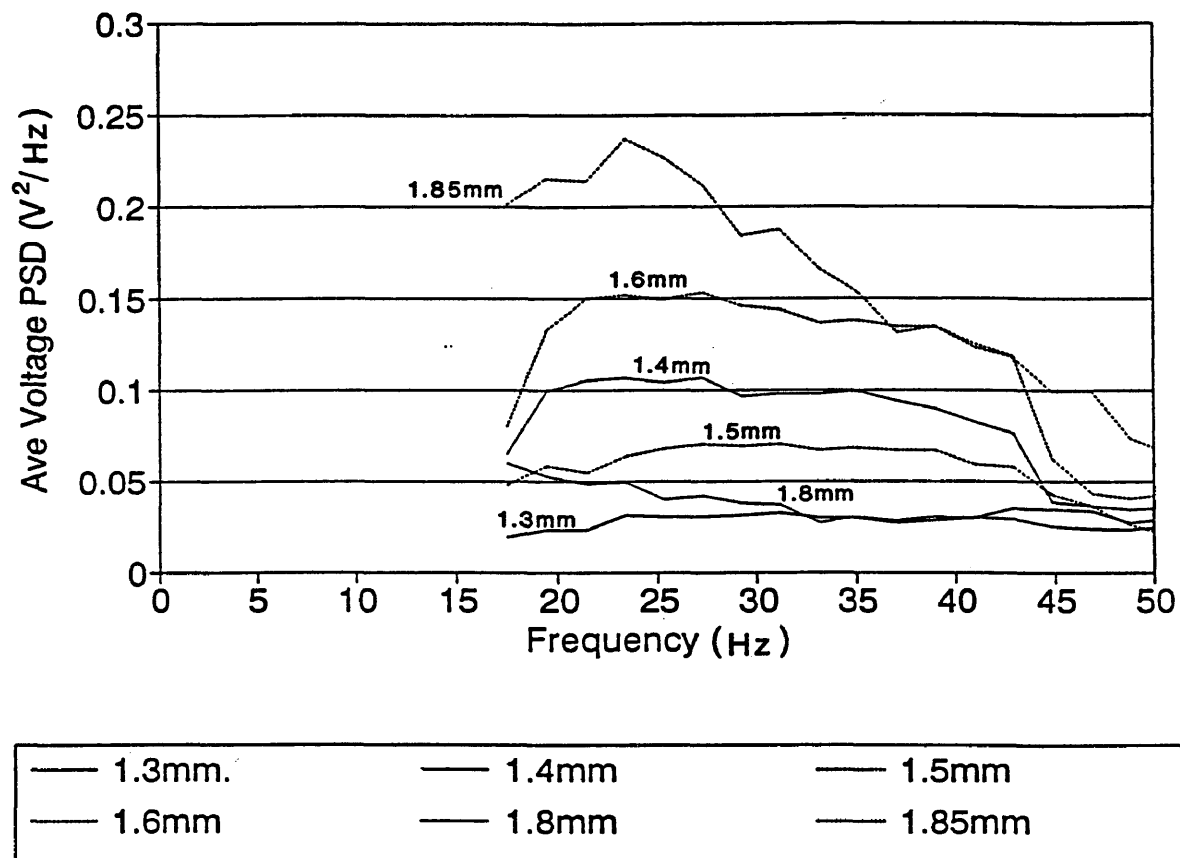


Figure 4.1.4 PSD Voltage - 0 to 50 Hertz for Varying Bore Diameter

4.1.3 Droplet Frequency Analysis. The droplet frequency was calculated counting the number of frames which passed during the development of 10 drops of molten electrode. Each frame was a thousandth of a second. Figures 4.1.5a and 4.1.5b, graph the droplet frequency and standard deviation versus bore diameter. The average droplet frequency increases

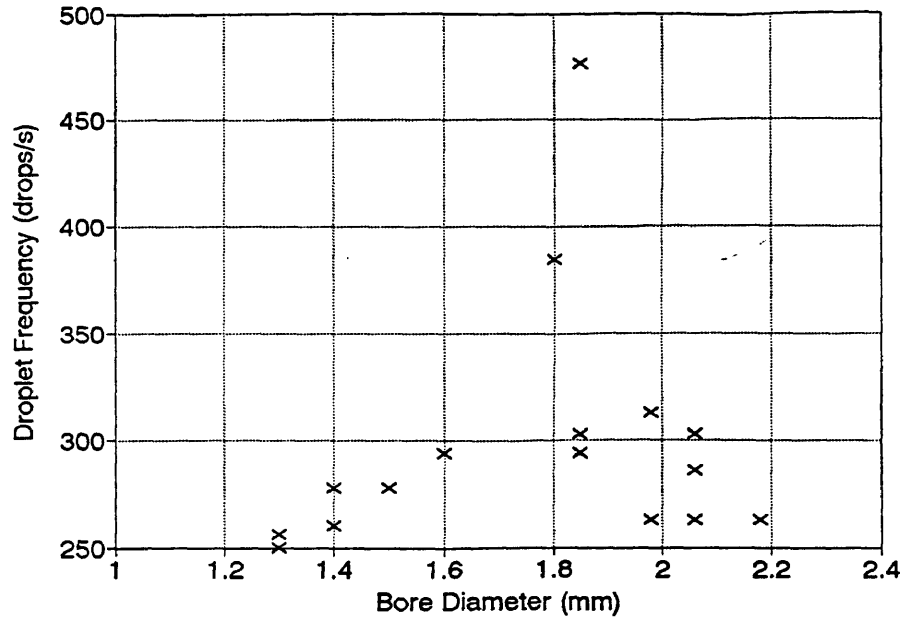


Figure 4.1.5a Droplet Frequency Versus Bore Size

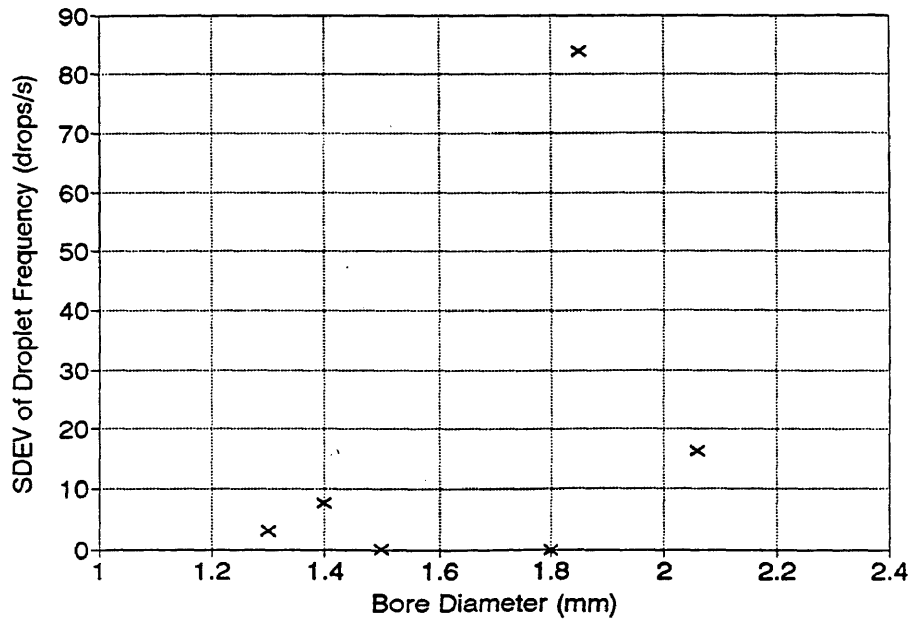


Figure 4.1.5b SDEV of Droplet Frequency Versus Bore Size

Figure 4.1.5 Droplet Frequency Characteristics Versus Bore Size

with bore size with a low SDEV until the bore diameter of 1.85 mm is reached, at which point the average droplet frequency and SDEV peak. From observation, all contact tubes had smaller secondary droplets along with a major droplet. The major droplets were counted to determine the plotted droplet frequency. The droplets changed in form from small discrete droplets with short necking of the electrode, to elongated droplets generating from a long narrow neck. Between 1.98 mm and 2.2 mm bore diameters the mode of transfer changed from discrete droplets to a stream of molten electrode, Figure 4.1.6. Current affects droplet transfer mode (Heald, 1991), and the increase in average current with bore diameter may explain the change in droplet formation.

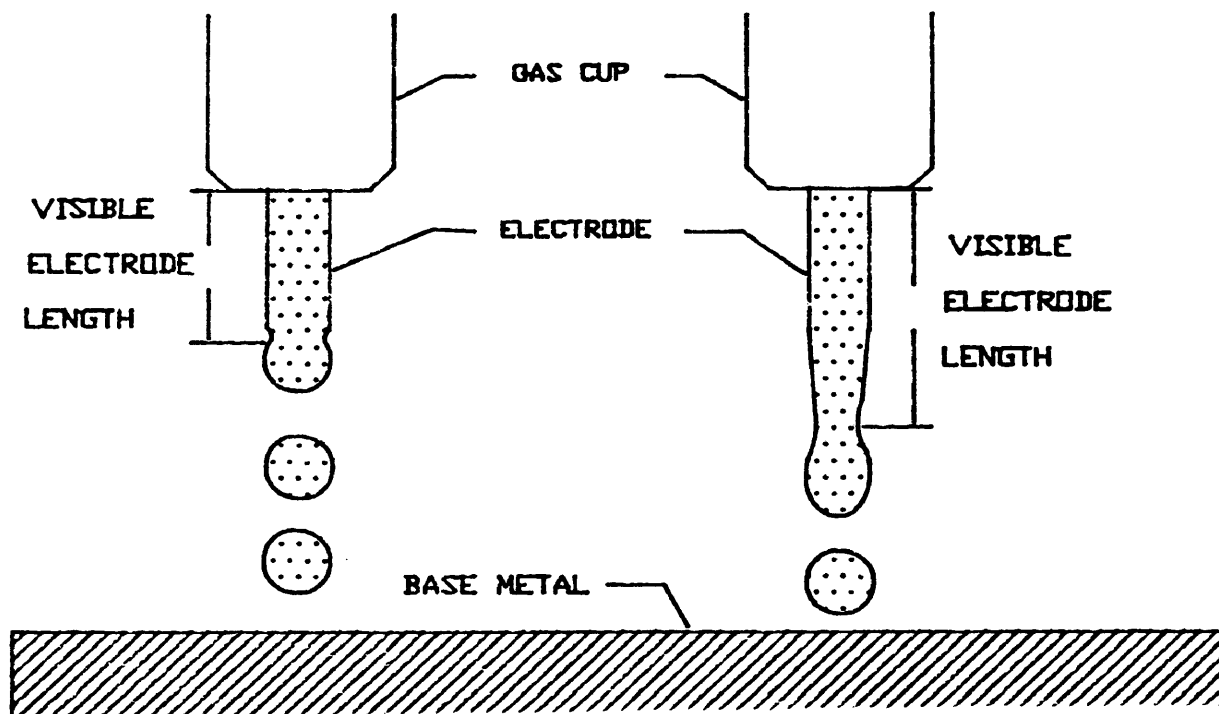


Figure 4.1.6 Droplet Profile with Enlarging Bore Size

4.1.4 Arc Length Analysis. Using the wire diameter 1.14 mm (.045") as a reference on the video monitor, the scale for the monitor was calculated as 5 mm = 1.14 mm. The extremes in arc length were calculated by measuring the visible electrode length for each tube. It was hoped that an increase in arc length would correspond to an increase in bore diameter. But as Figure 4.1.7 indicates no such correspondence appears on the graph.

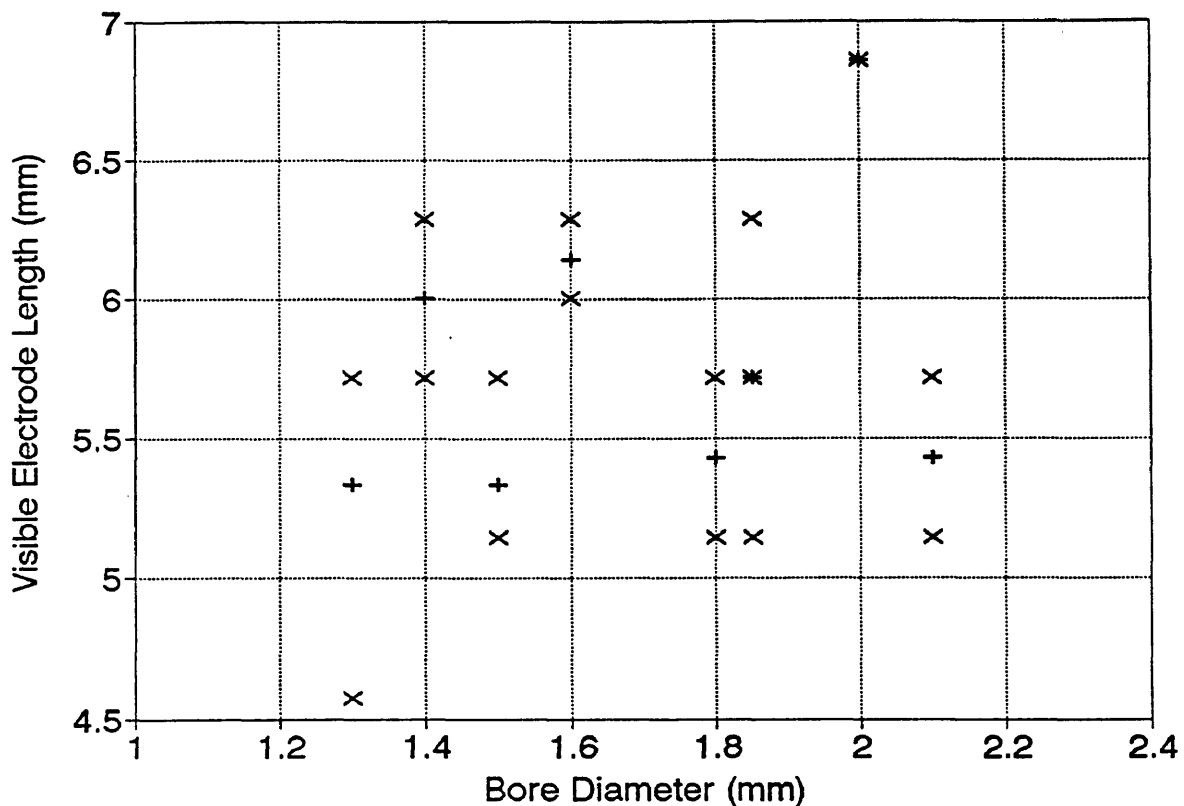


Figure 4.1.7 Range of Visible Electrode Length Versus Bore Size

4.1.5 Discussion of Simulated Wear Tests. The SDEV of droplet frequency may be of use in selecting an optimum ratio of contact tube diameter to electrode diameter for a constant potential GMAW process. The low standard deviations of droplet frequency occur with a contact tube to electrode diameter ratio less than 1.62 mm/mm, as shown in Figure 4.1.8.

The preferred droplet transfer mode occurs at a bore diameter less than 1.98 mm or a tube diameter to electrode diameter ratio of less than 1.73 mm/mm.

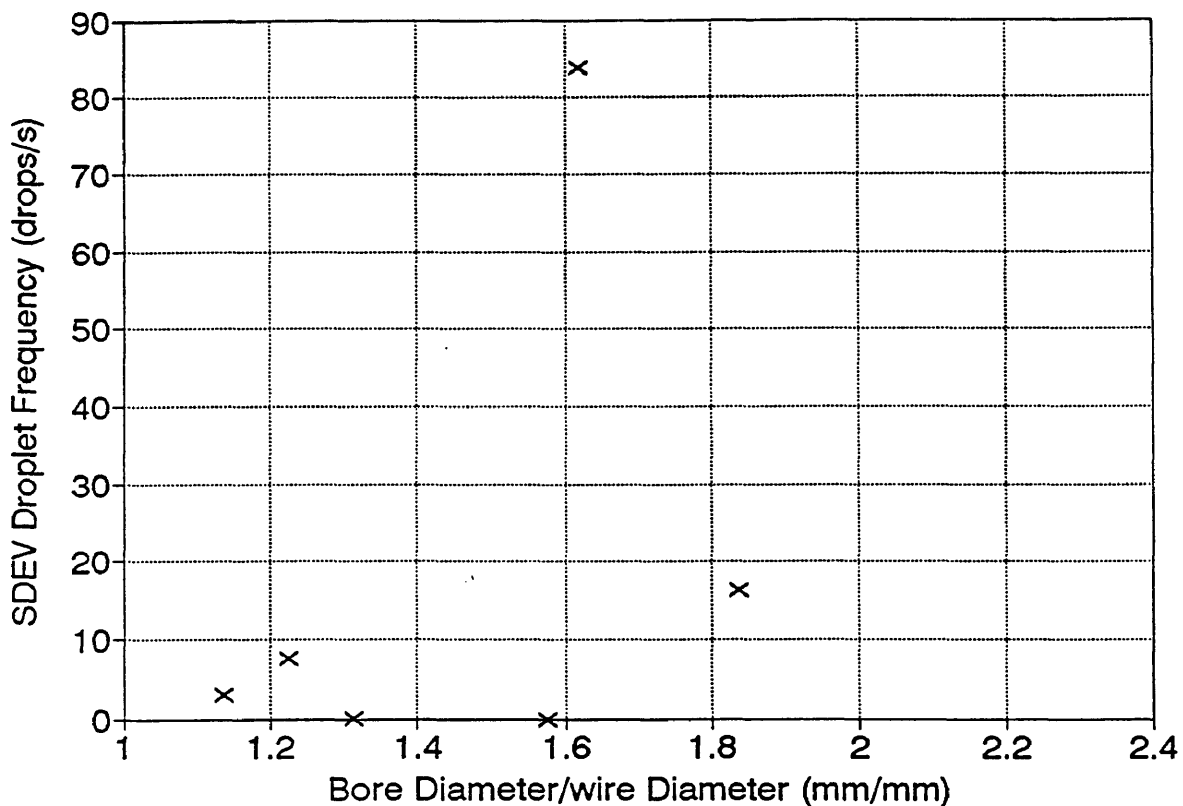


Figure 4.1.8 SDEV of Droplet Frequency Versus Ratio of Bore/Wire Diameters

## 4.2 Actual Wear Tests

4.2.1 Wear Test Group I. Group I used a curved torch, 10 Tweco L14-0.45 1.2 mm tubes and 95% argon - 5%O<sub>2</sub> shielding gas, see Table 4.2.1. Wire feed speed data (acquired at 2000 samples/s) was analyzed by counting the number of "outliers", points where the WFS exceeded a set limit. The limit was a multiple of the SDEV of wire feed speed and it was varied to find an increasing trend in the number of "outliers" with welding time.

TABLE 4.2.1

## Actual Wear Test - Group I

Tube Number	Welding Time (min)	Mean Amperage (Amperes)	Sample Rate Samples/sec	Comments
LW0	20	225	2000	E70S-3 wire did not operate properly
LW1	19	250	2000	Switched to ER100S-1 wire.
LW2	42	250	2000	Switched from 250 A to 225 A after 28 minutes
LW4	135	250	2000	Wire ran out at 135 minutes
LW10	48	220	200,2000	Wire ran out
LW11	62	220	200,2000	Leaky gas O-ring, moved contact tube, stopped welding

Note: Shielding Gas was 95% argon - 5%O<sub>2</sub>

This increasing trend in "outliers" appeared in the WFS data of contact tube LW4 with limit of 3 times the SDEV. Wire feed speed variations are a low frequency phenomena, therefore the acquisition rate was changed to include both 200 and 2000 samples/s for later tests in Group I. The "outliers" technique was not successful in providing a consistent rising trend relative to wear.

The analysis of the PSD curve for the arc voltage showed an increased area under the curve in the 0 to 4 Hertz frequency range for LW10 and LW11. An example of this event is shown in Figure. 4.2.1. It shows the actual voltage recorded during welding with a single contact tube. The envelope of the voltage appears more ragged as wear progresses, this variation was also observed in the arc during

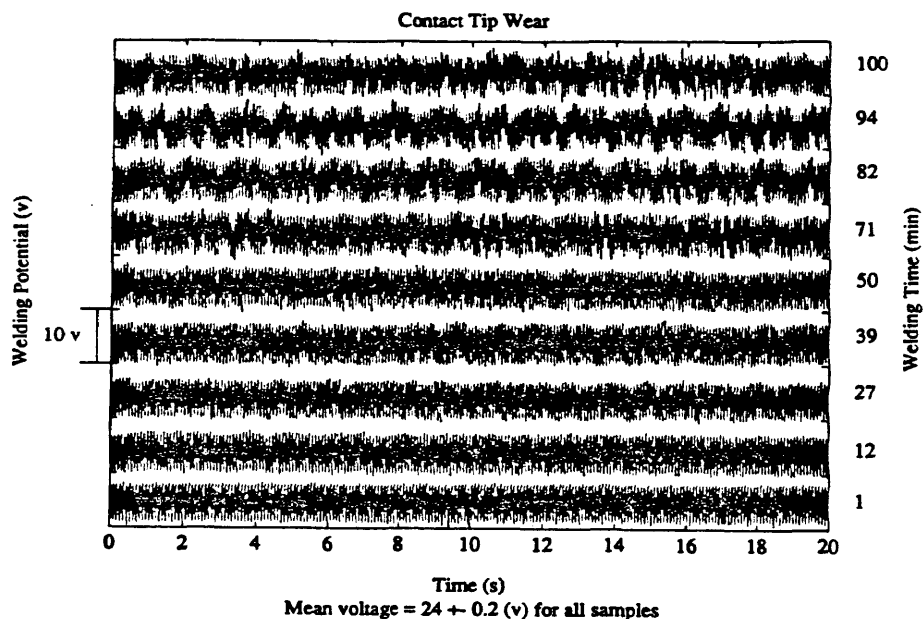


Figure 4.2.1 Voltage Signal with Increasing Weld Time

testing. As wear advanced, the arc became more erratic and at times appeared to pulse. The voltage (V) was sampled at time zero with a new contact tube at 200 cycles per second for a total of 90 seconds, and every 10 to 15 minutes thereafter. The voltage data was normalized according to

$$V' = \frac{V - \bar{V}}{\bar{V}}$$

where  $\bar{V}$  is the mean voltage and  $V'$  is the normalized voltage. Since the majority of voltage variance occurred in the 0 to 4 Hertz range, the power spectral density in this frequency range was calculated from the normalized data, PSDV. Then the area under the PSDV curve was approximated using the Riemann Summ. The area under the PSDV curve is the mean square voltage, MSV, Figure 4.2.2.

$$MSV = \sum_{i=0}^n = \left\{ \left( \frac{PSDV_i + PSDV_{i+1}}{2} \right) * \Delta f \right\}$$

The mean square voltage from 0 Hertz to 4 Hertz was normalized by dividing it by the mean square voltage at time zero. The normalized mean square voltage is called PSDA.

$$PSDA = \frac{MSV}{MSV_0}$$

The length of the electrode consumed was calculated by multiplying the average WFS by the welding time for each tube. Arc voltage was selected for further analysis.

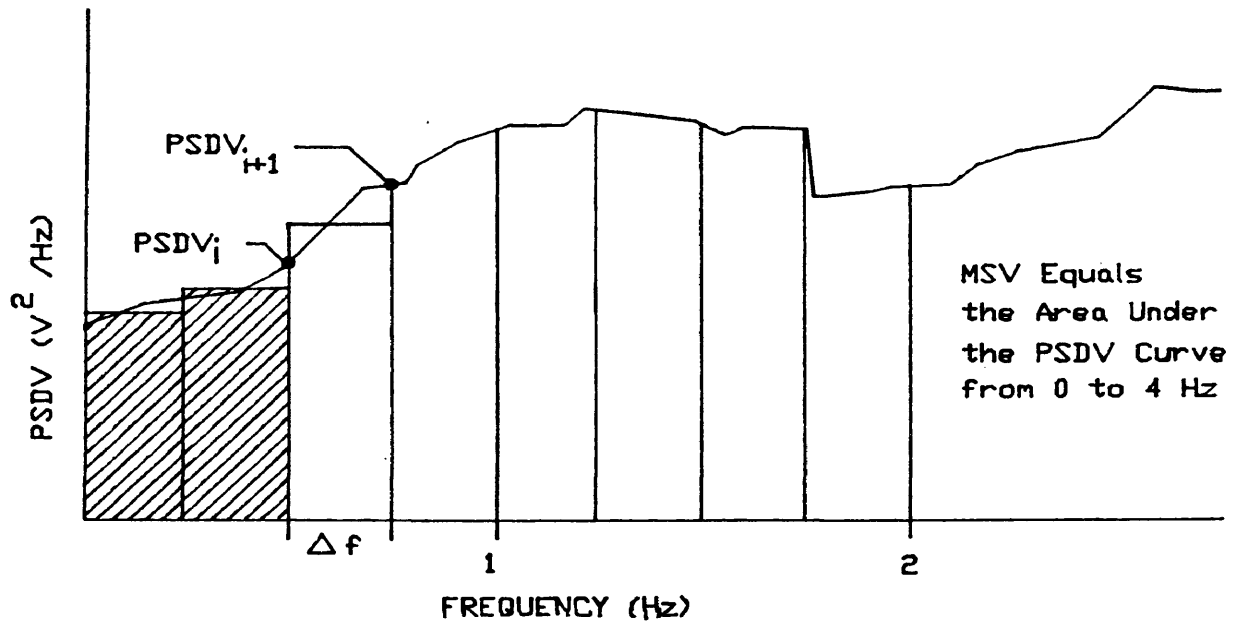


Figure 4.2.2 Mean Square Voltage

4.2.2 Wear Test Group II. Four Tweco 14 -.045 (1.2 mm) contact tubes were used in Group II, see Table 4.2.2.

TABLE 4.2.2  
Actual Wear Test - Group II

Tube Number	Welding Time (min)	Mean Amperage (Amperes)	Sample Rate Samples/sec	Comments
SW1	105	150	200,2000	95% argon - 5%O <sub>2</sub> shielding gas
SW2	99	150	200	Tube accidentally moved, stopped at 99 minutes
SW3	102	150	200	
SW4	140	220	200	SW4 used in weave test and bore was measured

Note: Shielding gas for SW2, SW3 and SW4 was 95% argon - 5% CO<sub>2</sub>.

Figure 4.2.3a and b show PSDA of arc voltage versus length of electrode consumed for contact tubes with different compositions and designs, different weld gases and different average amperages. The PSDA steadily increased, reaching a peak (PSDap) in all cases. After PSDap was attained, the wear parameter became erratic, leveling off or decreasing in value. PSDap can be identified in each case. However, before it can

be used as a wear monitor, it must be correlated with weld quality.

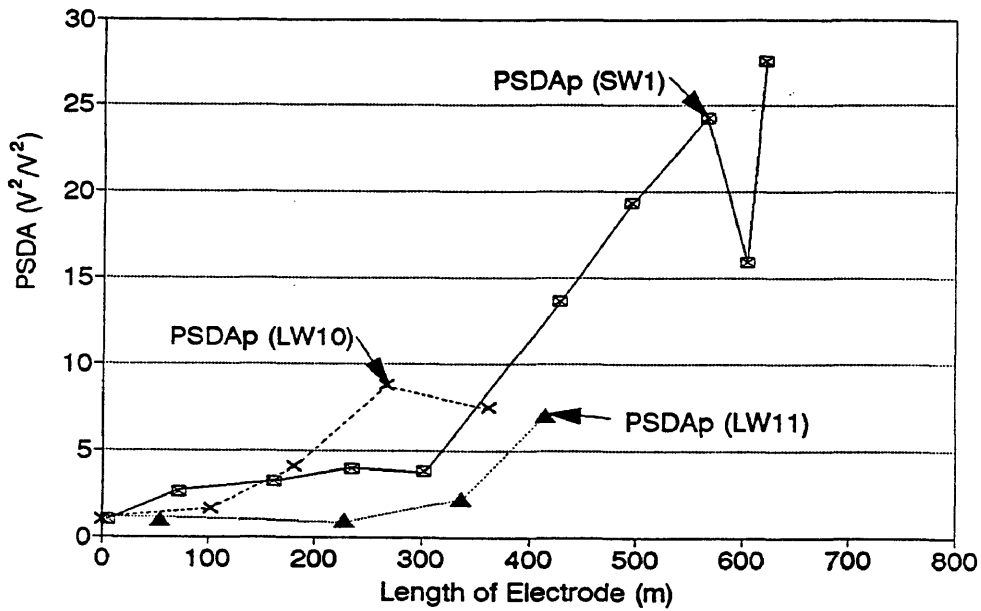


Figure 4.2.3a PSDA of Tubes LW10, LW11 and SW1

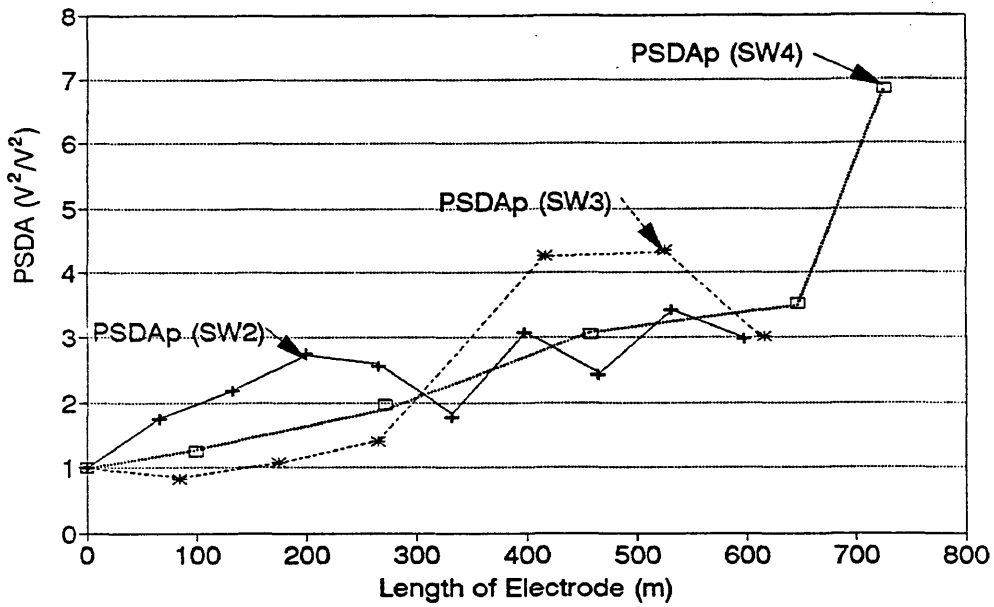


Figure 4.2.3b PSDA of Tubes SW2, SW3 and SW4

Figure 4.2.3 PSDA of Group I and Group II Versus Length of Electrode

4.2.3 Wear Test Group III. Group III used the same pulsed current power supply as Group I and II, but a straight Hobart torch and contact tubes were used, see Table 4.2.3. The amperage setting was increased to 300 A, in order to

TABLE 4.2.3

## Actual Wear Test - Group III

Tube Number	Welding Time (min)	Mean Amperage (Amperes)	Sample Rate Samples/sec	Comments
A1	252	300	200	Tube: Hobart model H17700 (C12200) 1.4 mm/.054"
A2	90	300	200	Hobart H17700
B1	418	300	200	Tube: Hobart model H177059 (C18100) 1.4 mm/0.054"
C1	90	300	200	Tube: Hobart model H379296 (C12200) 1.4 mm-1.6 mm / 0.054"-0.062"

Note: Shielding gas 95% argon - 5% CO<sub>2</sub>. Diameter measurements of worn bore were taken for A2, B1 and C1 tubes.

operate at the recommended upper limit for the welding conditions.

In Group III the PSDA and companion bore measurement were recorded for specific welding times. The initial bore diameter at time zero ( $D_0$ ) and the length of the elongated bore developed in the direction of the cast ( $D_m$ ) were measured and recorded. Cast is the curvature inherent in the electrode from wire drawing and winding onto the spool. All wound wire has a cast and whether a straight or curved torch is used, wear develops in the direction of the cast. Figure 4.2.3, is a typical wear pattern for a GMAW process.

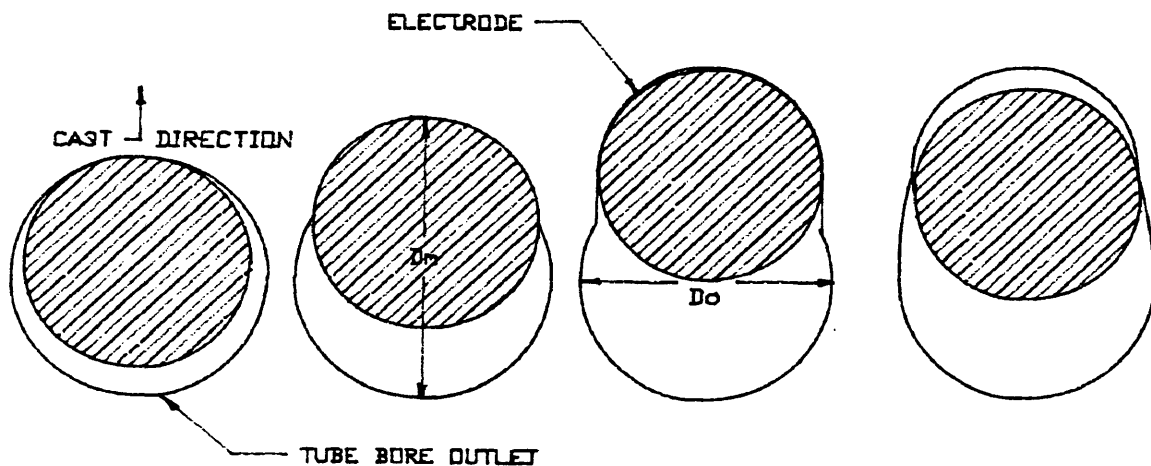


Figure 4.2.4 Wear Pattern for GMAW Process with Steel Electrode

The dimensionless wear ratio ( $R$ ) is created by dividing the enlarging diameter ( $D_m$ ) by the original bore diameter ( $D_o$ ). As the electrode is continuously fed through the contact tube, wear of the tube surface results in an ever larger bore outlet. Figures 4.2.5, 4.2.6, 4.2.7 and 4.2.8 show changes in PSDA and  $R$  ( $D_m/D_o$ ) with the increasing length of electrode fed through the tube during welding, for Group III and S4. The peak PSDA value ( $PSDA_p$ ) is identified in each graph. The wear ratio which occurs at the same time  $PSDA_p$  is reached is labeled  $R_p$ . The wear ratio  $R_p$  is not the peak wear ratio, it is the wear ratio which corresponds to the point at which the largest area under the power spectral density curve is reached ( $PSDA_p$ ). For the straight welding torch,  $R_p$  falls within a range from 1.44 to 1.55.

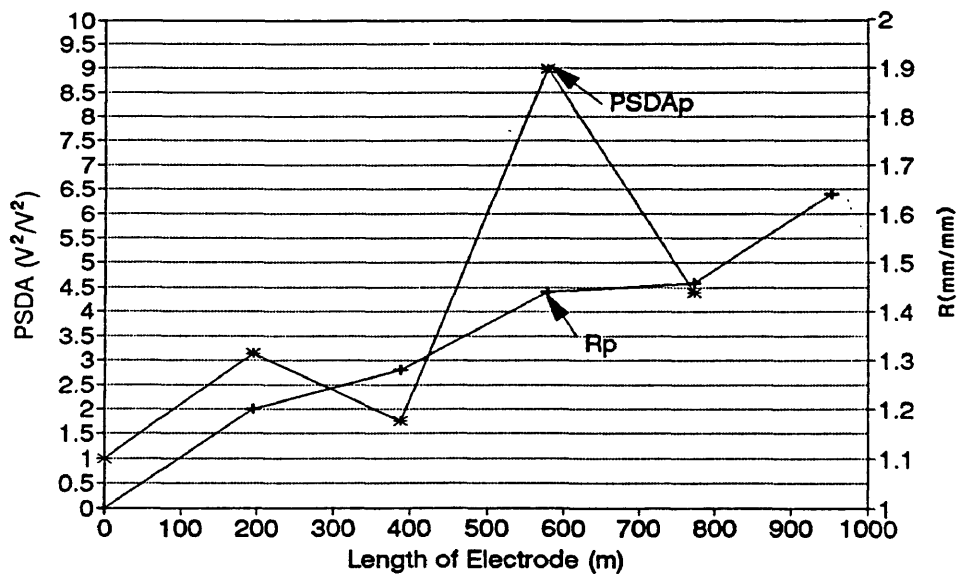


Figure 4.2.5 PSDA and  $R$  ( $D_m/D_o$ ) Versus Length of Wire Fed for (Tube A2)

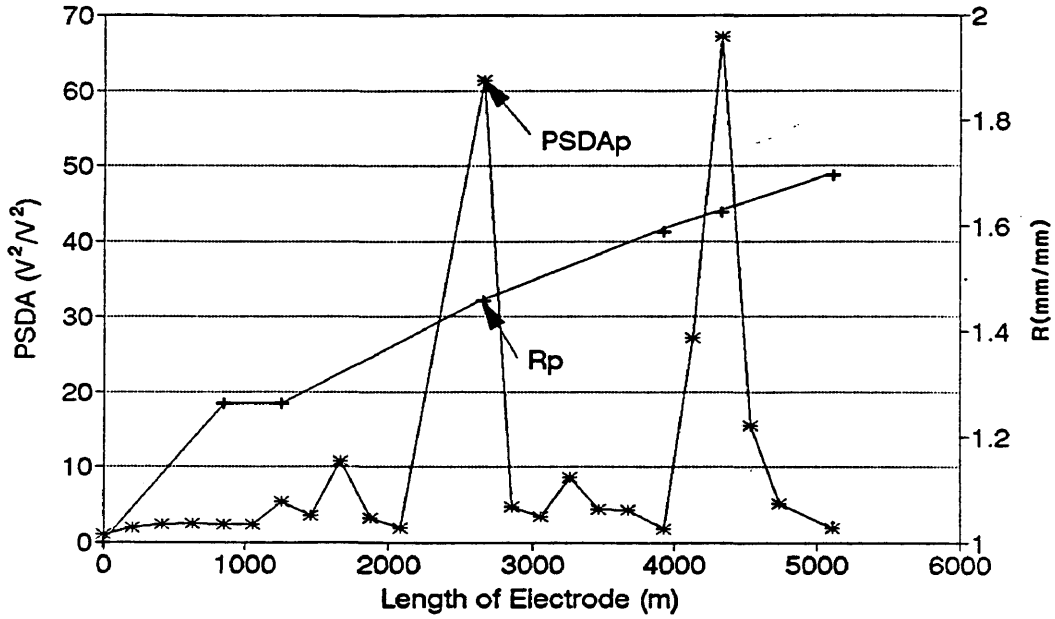


Figure 4.2.6 PSDA and R ( $D_m/D_o$ ) Versus Length of Wire Fed for (Tube B1)

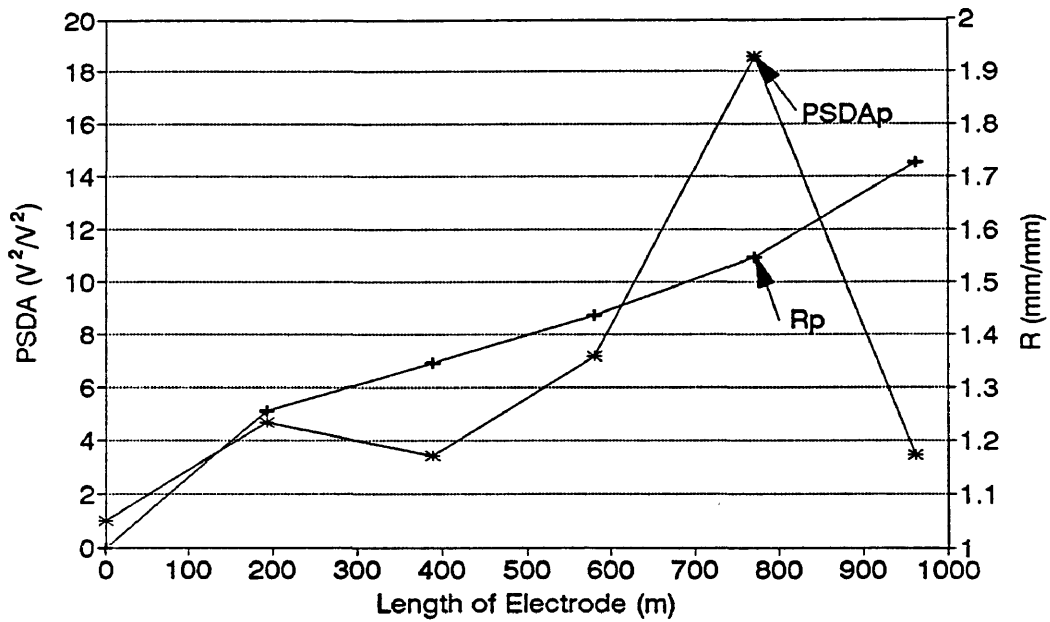


Figure 4.2.7 PSDA and R ( $D_m/D_o$ ) Versus Length of Wire Fed for (Tube C1)

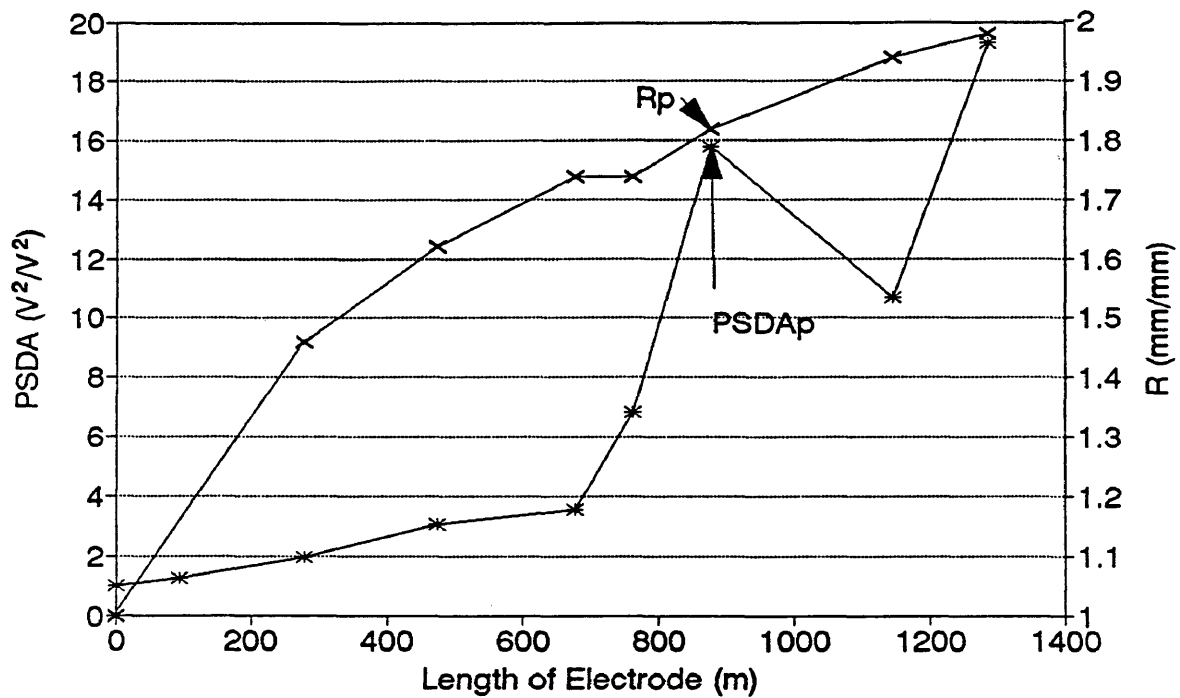


Figure 4.2.8 PSDA and  $R$  ( $D_m/D_o$ ) Versus Length of Wire Fed for (Tube S4)

4.2.4 Sectioned Contact Tubes. Tubes A2, B1, C1 and S4 were cut longitudinally, perpendicular to the direction of wear. The areas of erosion and adhesion were detected and measurements taken with an image analyzer [LECO Model 2001], Table 4.2.4.

TABLE 4.2.4  
Contact Tube Measurements

Tube Number	Wear Length (mm)	Adhesion Length (mm)	Calculated Approach Angle $\alpha$ (degrees)
A2	15.32	1.754	.0533
B1	16.07	1.564	.0531
C1	12.89	1.910	.0787
S4	14.10	8.540	.0880

Figure 4.2.9 shows the contact tube section which is perpendicular to the direction of wear, along with the wear and adhesion area, for tubes A2, B1, C1 and S4.

4.2.5 Discussion of Actual Wear Tests. To determine a relationship between PSDAp and Rp, the following were calculated; the change in tube exit contact length, contact surface area between the electrode and the contact tube during welding, and the volume of worn copper in relation to the angle of approach ( $\alpha$ ) and Dm. Figure 4.2.10 displays the geometric relationship between the electrode and the contact tube during the welding process. As the weld progresses the electrode wears away the outlet of the contact tube in the direction of cast. The wearing process continues until the electrode has worn a notch, equal to its radius, into the tube

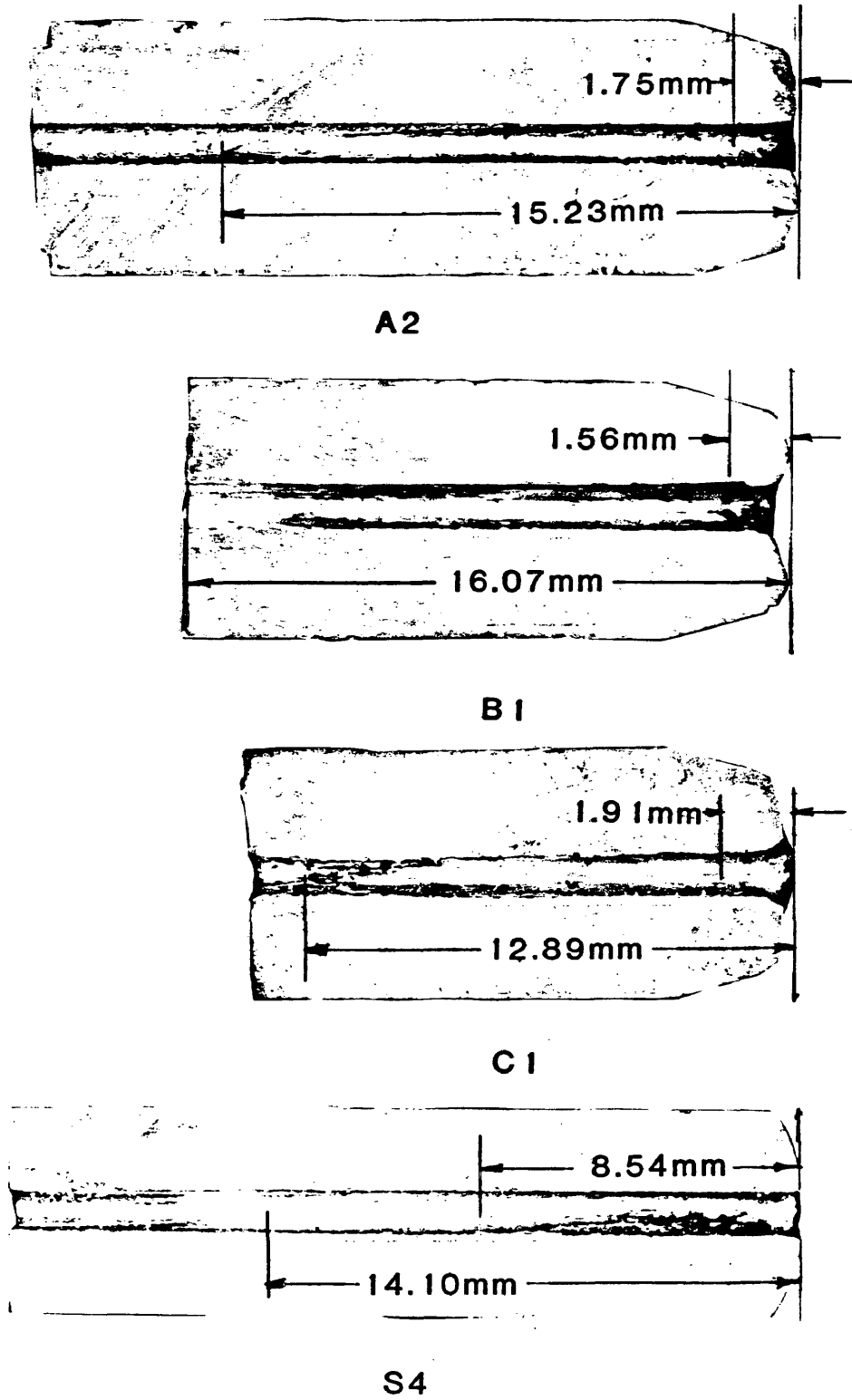


Figure 4.2.9 Sectioned Contact Tubes

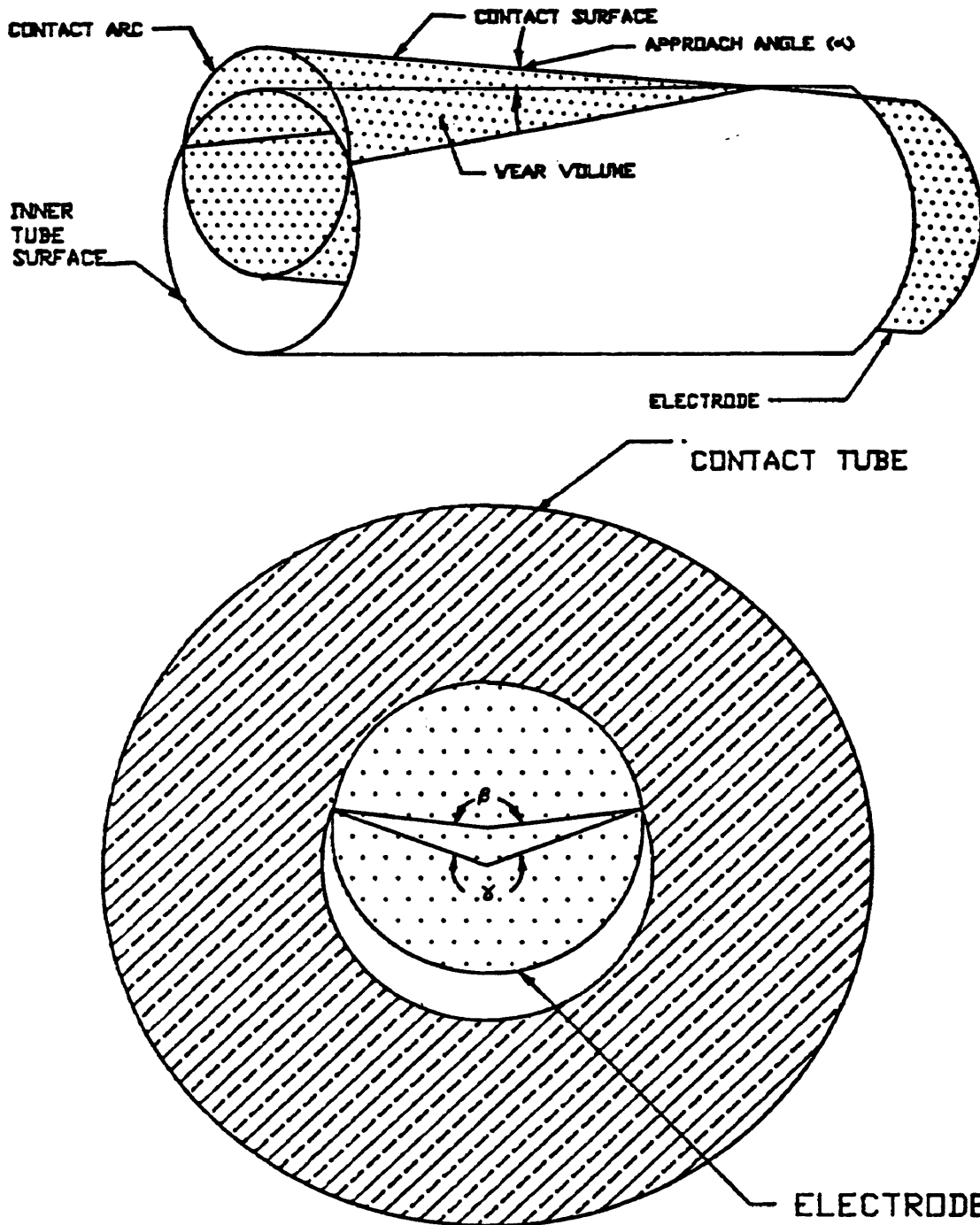


Figure 4.2.10 Electrode and Tube Wear Configuration

( $\beta = 180^\circ$ ). At this point in time, the line contact at the exit between the electrode and the tube has reached a maximum, and the wear volume rate decreases. The wear volume rate changes because the line contact reaches its maximum value, Figures 4.2.11a,b and c. This occurrence closely corresponds to a peak PSDA (for A2, B1 and C1 with a straight weld torch) at R equal to 1.47 mm/mm.

One hypothesis for contact tube wear is called the electrode extension effect. That is, as wear progresses the point of current transfer can move within the electrode-tube contact surface area, which is greater for a smaller approach angle ( $\alpha$ ). The voltage variance is produced by the changes in the voltage drop across the electrode extension and would continuously increase as contact surface area increases.

Yamada & Tanaka (1987) determined that the point of current transfer is confined to the bottom one-fourth of the contact tube and that current passes to the electrode without sparking. The voltage variance would be a function of surface contact area and it is not necessarily a low frequency process. If surface contact area was the only factor, tubes tested with the straight torch would have PSDA values greater than tubes with the curved torch, because the approach angle is less and contact surface area is greater for the depth of wear. The results of wear tests in this report do not indicate this.

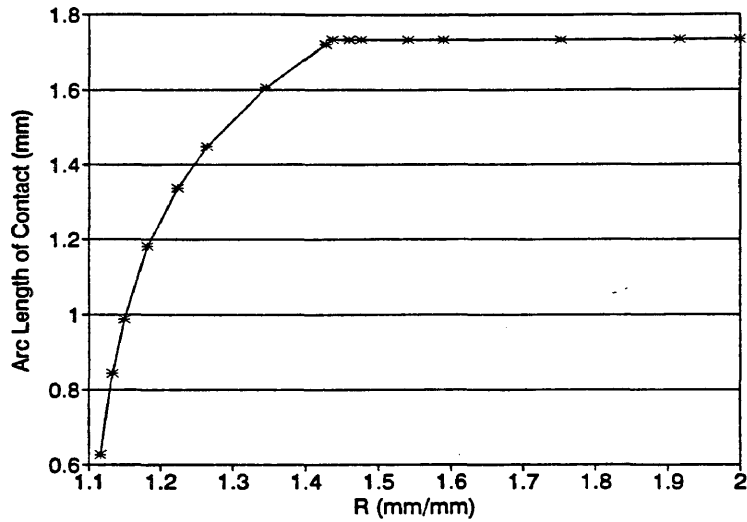


Figure 4.2.10a Arc Length of Contact Versus R (Dm/Do)

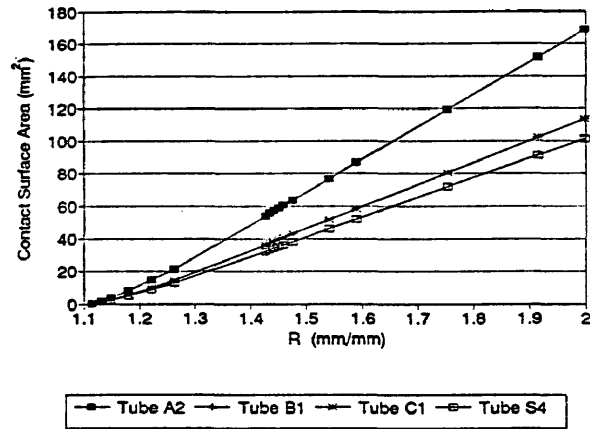


Figure 4.2.10b Contact Area Versus R (Dm/Do)

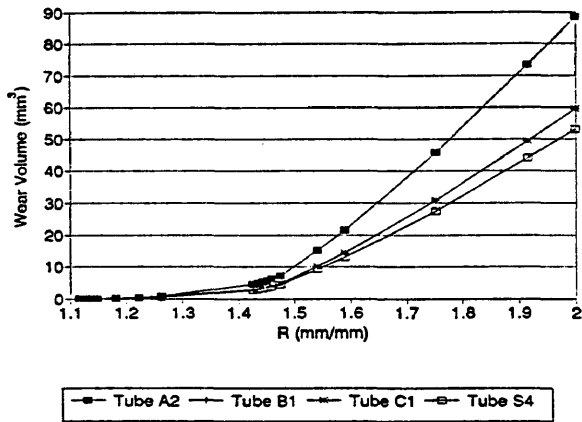


Figure 4.2.10c Wear Volume Versus R (Dm/Do)

Figure 4.2.10 Configuration Parameters Versus Rm (Dm/Do)

The contact tube used in the curved torch, S4, has a larger ratio of adhesion area to surface contact area than the tubes used in a straight torch. Therefore, other factors, such as contact pressure, may affect the actual adhesion area.

The low frequency voltage variance in a GMAW process with a pulsed-current power source and feed-back control of the WFS, develops from a combination of electrode extension variations and fluctuation in WFS due to adhesion. As mentioned earlier, adhesion (cold welding and hot welding) between the surfaces of the electrode and tube creates a junction which can be destroyed by the sliding motion of the electrode. Because the tube material is eroded with weld time, junction failure at the tube surface is the major area of separation.

When WFS is interrupted due to an adhesive bond, arc voltage increases, sending a signal to the wire feed motor to increase speed. As soon as the adhesive bond fails, the WFS is no longer restricted, but the controller has already recommended an increase in speed. The combined rise in speed lengthens the electrode extension and shortens the arc length. Then the controller signals the wire feed motor to decrease speed. This cycle is affected by the control system, dynamics of the feeder motor and frequency of adhesive bonds.

The maximum variance of the arc voltage (PSDAp) at these low frequencies coincides with the point of maximum line contact at the exit of the tube and at the decrease in the rate of wear volume. If current transfer is limited to the extreme tip of the tube, the probability of adhesive bonds forming depends upon the line of physical contact between the electrode and the tube. The low frequency changes in WFS are the consequence of increased frequency of adhesive contact between the electrode and the tube due to the enlarging line contact.

4.2.6 Buckingham Pi Theorem. The Buckingham Pi Theorem was employed in an attempt to quantify relationships between the PSD data and other selected welding parameters. PI1, PI2, PI3 and PI4 were developed in the following manner:

- Step 1. List the parameters involved.
- Step 2. Select a set of fundamental (primary) units. Ampere was selected over Coulomb.
- Step 3. List the dimensions of all parameters in terms of primary units.
- Step 4. Select from the list of parameters five repeating parameters which include all the primary dimensions.
- Step 5. Set up dimensional equations combining the five selected repeating parameters with the remaining parameters to form dimensionless groups, (Fox & McDonald, 1978).

TABLE 4.2.5  
Buckingham PI Theorem

---

List of Parameters

<i>Parameter</i>	<i>Symbol</i>		<i>Units</i>	<i>Primary Units</i>
<i>Wear</i> (0-4 Hertz)	<i>W</i>	$V^2$	$(\frac{Kg\ m^2}{A\ S^3})$	$(\frac{M^2\ L^4}{A^2\ t^6})$
<i>Current</i>	<i>I</i>	<i>A</i>	<i>A</i>	(A)
<i>Tube Diameter</i>	<i>Do</i>	<i>m</i>	<i>m</i>	(L)
<i>Major Tube Diameter</i>	<i>Dm</i>	<i>m</i>	<i>m</i>	(L)
<i>Temperature</i>	<i>T</i>	<i>T</i>	<i>T</i>	(T)
<i>Specific Heat</i>	<i>Cp</i>		$(\frac{Kg\ m}{s^2}\ \frac{m}{Kg\ C})$	$(\frac{L^2}{t^2\ L})$
<i>Hardness</i>	<i>H</i>	$\frac{N}{M^2}$	$(\frac{Kg\ m}{s^2\ m^2})$	$(\frac{M}{t^2\ L})$
<i>Weld Time</i>	<i>tw</i>	<i>t</i>	<i>t</i>	(t)
<i>Total Energy</i>	<i>E</i>	$\frac{I\ V}{m/s}$	$(\frac{Kg\ m^2}{A\ S^3}\ \frac{A}{m/s})$	$(\frac{M\ L}{t^2})$

Note: From the nine welding parameters, I, Do, Cp, H, and tw are selected as the repeating parameters. The primary units are: Mass, Length, Temperature, time and Current.

## Calculation of PI1, PI2, PI3 &amp; PI4

$$(Cp)^a (H)^b (Do)^c (I)^d (tw)^e W = (MLTtA)^0$$

$$\left(\frac{L^2}{t^2 T}\right)^a \left(\frac{M}{t^2 L}\right)^b (L)^c (A)^d (t)^e \left(\frac{M^2 L^4}{A^2 t^6}\right) = (MLTtA)^0$$

$$M: b + 2 = 0$$

$$L: 2a - b + c + 4 = 0$$

$$T: -a = 0$$

$$t: -2a - 2b + e - 6 = 0$$

$$A: d - 2 = 0$$

$$a = 0, b = -2, c = -6, d = 2, e = 2$$

$$PI1 = \left(\frac{W I^2 tw^2}{H^2 Do^6}\right)$$

$$(Cp)^f (H)^g (Do)^h (I)^i (tw)^j Dm = (MLTtA)^0$$

$$\left(\frac{L^2}{t^2 T}\right)^f \left(\frac{M}{t^2 L}\right)^g (L)^h (A)^i (t)^j L = (MLTtA)^0$$

$$M: g = 0$$

$$L: 2f - g + h + 1 = 0$$

$$T: -f = 0$$

$$t: -2f - 2g + j = 0$$

$$A: i = 0$$

$$f = 0, g = 0, h = -1, i = 0, j = 0$$

$$PI2 = \left(\frac{Dm}{Do}\right)$$

## Calculations Continued

$$(Cp)^k (H)^1 (Do)^m (I)^n (tw)^p T = (MLTtA)^0$$

$$\left(\frac{L^2}{t^2 T}\right)^k \left(\frac{m}{t^2 L}\right)^1 (L)^m (A)^n (t)^p T = (MLTtA)^0$$

$$M: l = 0$$

$$L: 2k - l + m = 0$$

$$T: -k + 1 = 0$$

$$t: -2k - 2l + p = 0$$

$$A: n = 0$$

$$k = 1, l = 0, m = -2, n = 0, p = 2$$

$$PI3 = \left(\frac{T Cp tw^2}{DO^2}\right)$$

$$(Cp)^{a''} (H)^{b''} (Do)^{c''} (I)^{d''} (tw)^{e''} E = (MLTtA)^0$$

$$\left(\frac{L^2}{t^2 T}\right)^{a''} \left(\frac{M}{t^2 L}\right)^{b''} (L)^{c''} (A)^{d''} (t)^{e''} \left(\frac{M L}{t^2}\right) = (MLTtA)^0$$

$$M: b'' + 1 = 0$$

$$L: 2a'' - b'' + c'' + 1 = 0$$

$$T: a'' = 0$$

$$t: -2a'' - 2b'' + e'' - 2 = 0$$

$$A: d'' = 0$$

$$a'' = 0, b'' = -1, c'' = -2, d'' = 0, e'' = 0$$

$$PI4 = \left(\frac{E}{H DO^2}\right)$$

The numbers used for Current, Temperature, Specific Heat and Hardness were assumed constant.

TABLE 4.2.6  
Buckingham Pi  
Constants

Parameter	Constant	Comments
Amperage	300 A 220 A	A2, B1, C1 S4
Temperature	1080°C	All tubes
Specific Heat	385 J/kg K	All tubes
Hardness	64HRF 59HRF	A2, C1, S4 B1

Note: (Brandis, 1983) HRF; Rockwell Hardness test F.

By following the Buckingham Pi Theorem, dimensionless relationships are developed from the selected parameters. By analyzing the graphs of PI1 versus PI2, PI3 and PI4, it can be determined which parameters have an effect on W, the means square voltage (MSV) from 0 to 4 Hz. It is desirable to have all data points fall within a narrow band. The data from Figures 4.2.12,13 and 14, show a close grouping for contact tubes A2, C1 and S4. Tube B1 does not fall within this grouping; indicating that additional parameters should be included in the analysis. The additional parameters selected

would reflect the superior wear resistance of tube B1. Tube B1 is made from a different copper alloy (C18100) and tolerates a longer weld time and corresponding length of electrode fed through the contact tube before PSDAp and Rp were reached, Figure 4.2.6. Hardness was selected as the Buckingham Pi parameter which indicated material composition, however that parameter proved to be insufficient.

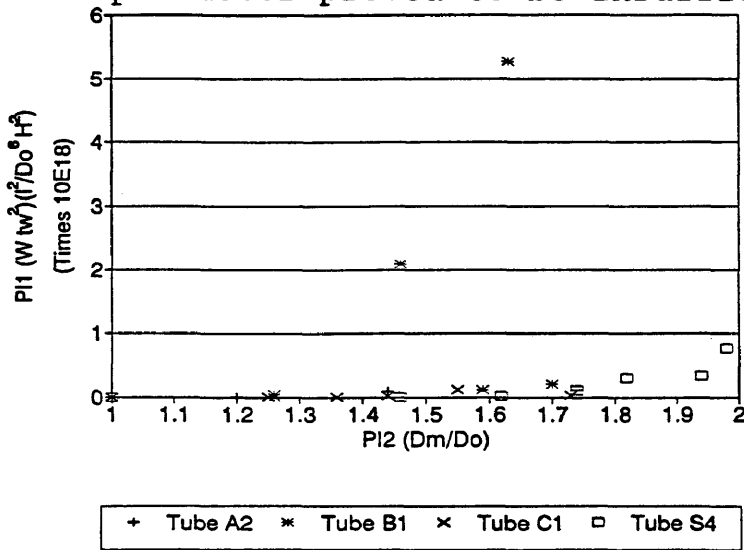


Figure 4.2.12 Buckingham Pi Theorem PI1 Versus PI2

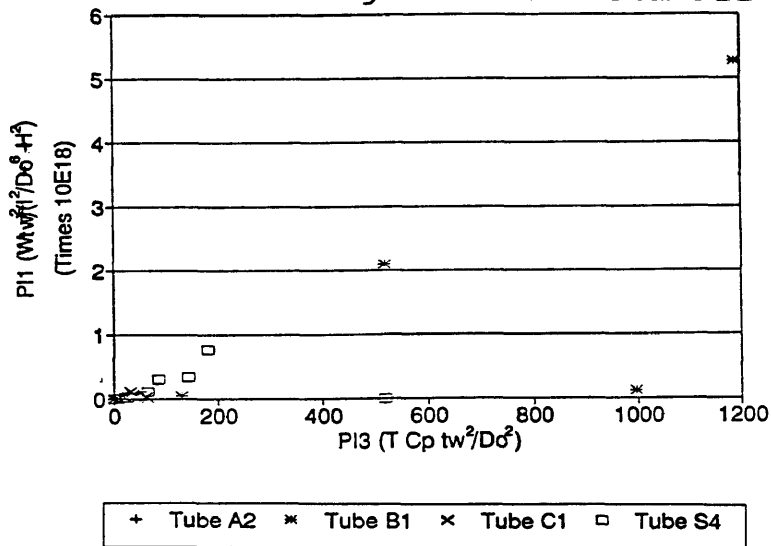


Figure 4.2.13 Buckingham Pi Theorem PI1 Versus PI3

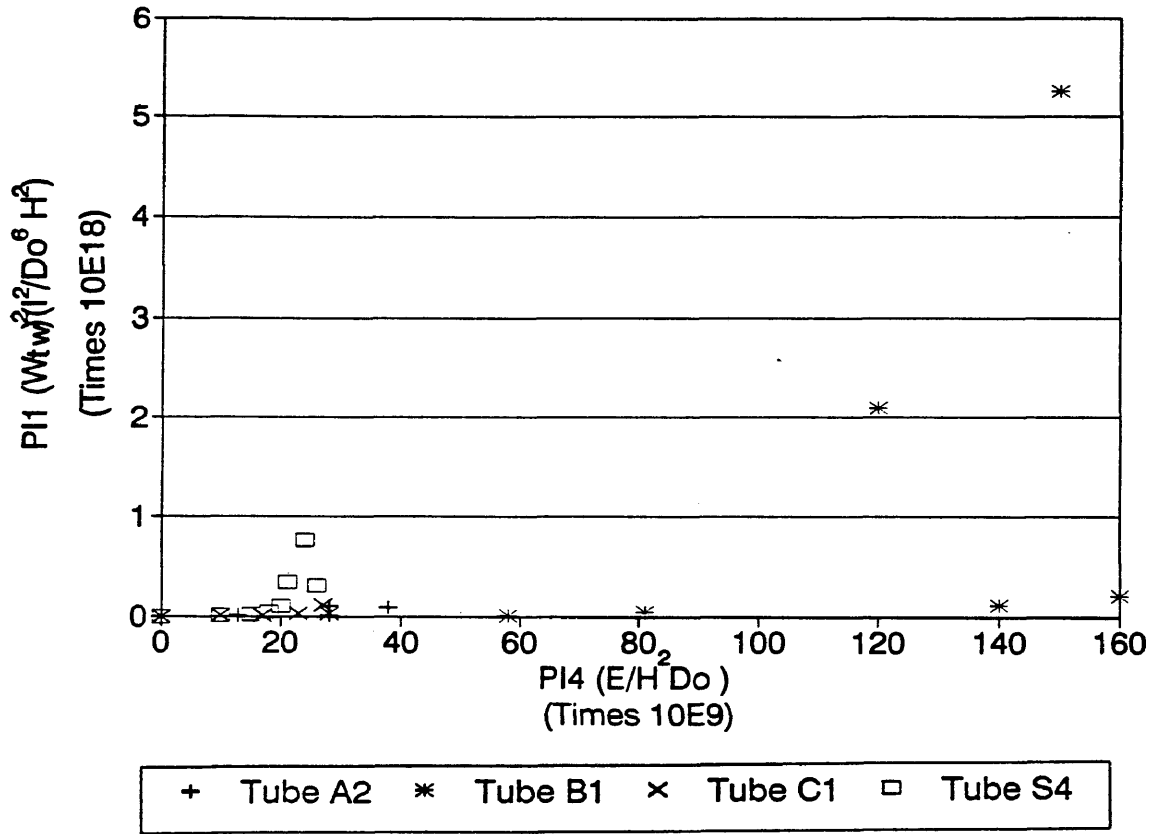


Figure 4.2.14 Buckingham Pi Theorem PI1 Versus PI4

### 4.3 Weave Test

The welding test for tube S4, included testing with a 1 Hertz weave imposed on the weld data. Test welds alternated between a straight weld (stringer bead) and a weave bead. Figure 4.3.1, displays the power spectral density of voltage for a stringer bead collected at time zero and the weave bead data collected at 3 minutes.

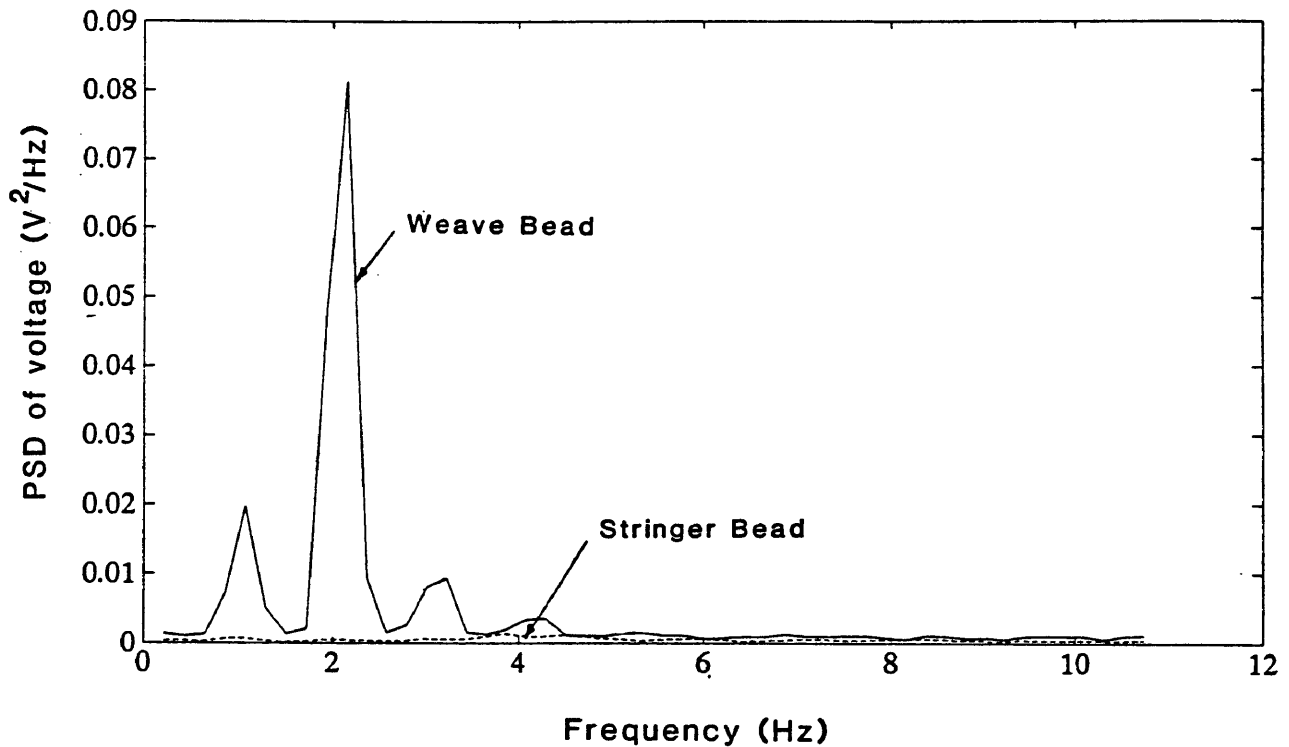


Figure 4.3.1 PSD Voltage for Stringer and 1 Hz Weave Bead at Time 0 and 3 minutes

Spikes at 1 Hertz and at multiples of the weave frequency are formed by applying the Fast Fourier Transform to the voltage signal which is full-wave rectification of a sine wave developed by the geometry of the groove, Figure 4.3.2.

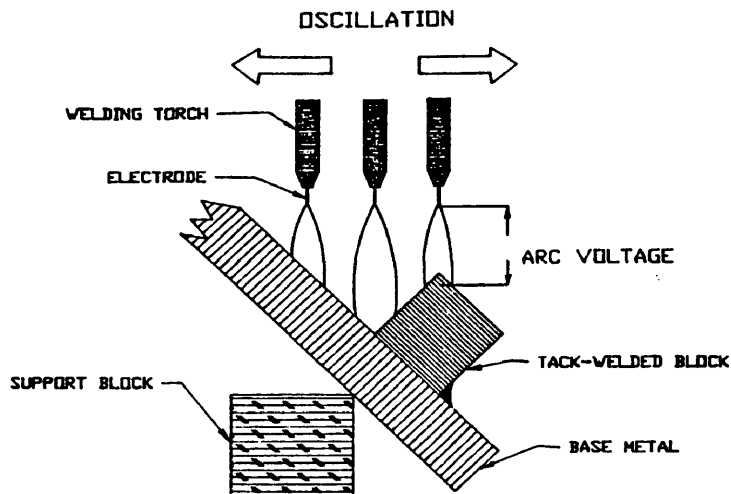


Figure 4.3.2a Weave Geometry

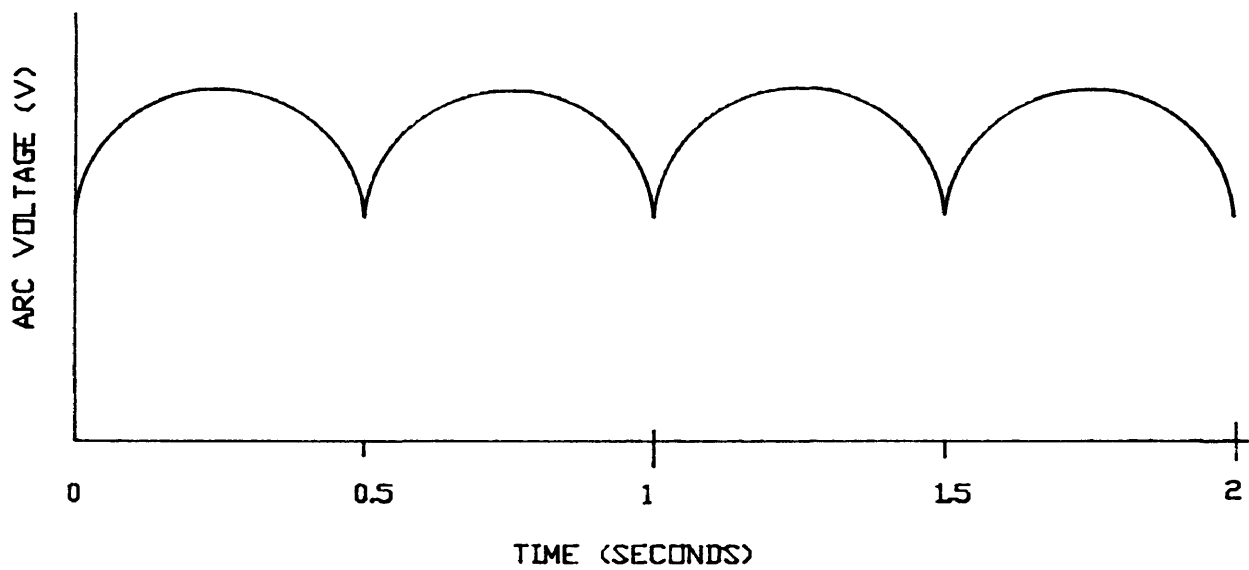


Figure 4.3.2b Weave Voltage Signal

Figure 4.3.2 Weave Geometry and Voltage Signal

Figure 4.3.3 shows the PSDA for the stringer test weld and the 1 Hz weave test weld. The PSDA for a weave bead can presently be used as a wear monitor only if welding conditions

are kept constant. Welding a weave bead along a skewed path or filling a groove with multiple passes, creates variations in the frequency and magnitude of the weave voltage data (Cooke et al. 1986).

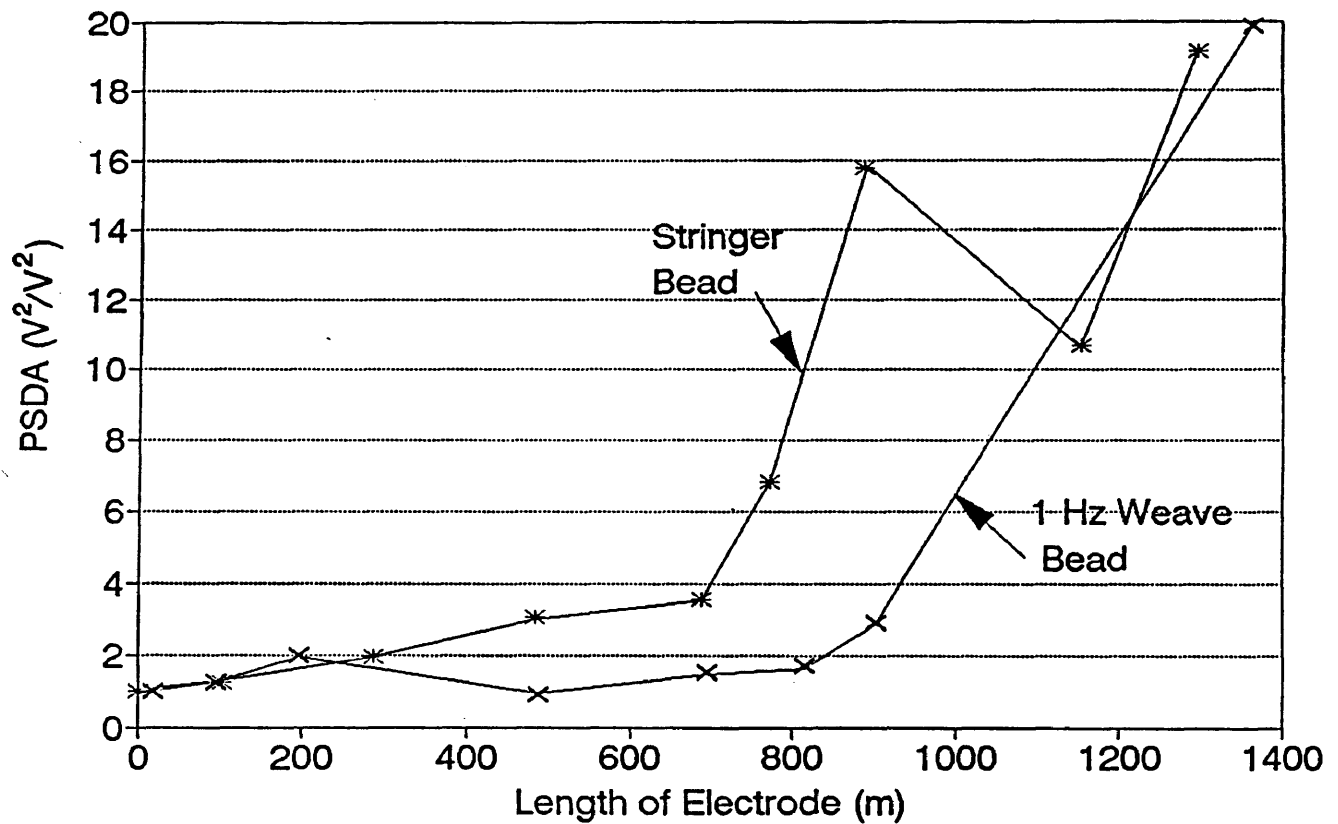


Figure 4.3.3 PSDA Versus Length of Electrode for Stringer & Weave Tests

## Chapter 5

### CONCLUSIONS

Through-the-arc sensing can detect contact tube wear. From these experiments it has been shown that the variance of the welding voltage correlates to contact tube wear.

The simulated wear tests indicate that a contact tube to electrode bore ratio of less than 1.6 would provide a droplet transfer mode with low standard deviation of droplet frequency, thus providing consistent weld characteristics.

Isolating a through-the-arc welding characteristic to monitor wear of the contact tube has been accomplished with the analysis of the power spectral density data for the welding voltage. Based on limited observations, the area under the power spectral density curve from 0-4 Hertz (PSDA) for a pulsed-current GMAW process can be used to observe wear of a contact tube. However, while the tube is in use, welding conditions such as, contact-tube-to-work distance, CTWD, and average welding current, must remain constant. In addition, low frequency perturbations, such as tracking drift, or a weave may alter the PSDA to the base PSDA developed during the initial weld, thus requiring that the monitoring technique be re-evaluated.

The PSDA identifies a point in the weld process, when the voltage variance has reached a maximum, and the electrode has

reached the maximum arc contact length with the contact tube. If weld quality is defined as (1) electrode positioning tolerance (2) maximum low frequency voltage variance or (3) bead width variance; then the area under the low frequency power spectral density curve or mean square variance of low frequency voltage (PSDA) can be used in identifying weld quality.

## Chapter 6

### SUGGESTIONS FOR FUTURE STUDIES

Since the majority of welding in the United States is performed with a constant voltage power supply, continued investigation of contact tube wear with a constant voltage power source would greatly benefit the welding industry.

Further study of the effects of contact tube wear on low frequency power spectral density data, electrode positioning, electrode - tube alloy combinations, current variations and bead width variance would further correlate a wear parameter with weld quality.

## REFERENCES CITED

(ASYST, 1988)

Asyst Software Technologies, Inc., 100 Corporate Woods,  
Rochester, N.Y. 14623 phone (716-272-0070).

(AWS Welding Handbook, 1991)

American Welding Society (AWS), 1991. Welding Handbook;  
Welding Processes. Ed. R. L. O'Brien. 8th ed. Vol 2.  
Miami, Fla.: AWS.

(Bendat & Piersol, 1971)

Bendat & Piersol, 1971. Random Data: Analysis and Measurement  
Procedures, Wiley-Interscience, N.Y.

(Brandis, 1983)

Brandis, Eric A., 1983 Smithells Metals Reference Book. 6th  
Ed. Butterworths.

(Cook et al, 1986)

Cook, G., Randel, M., Shepard, M., Yizhang, L. 1986.  
Adaptive Submerged Arc Welding Control. International  
Conference on Trends in Welding Research, ed. S.A. David,  
18-22. ASM Int. Joining Division Council, Gatlinburg,  
Tenn.

(Fox & McDonald, 1978)

Fox, R. and McDonald, A. T. 1978. Introduction to Fluid  
Mechanics. John Wiley & Sons, Inc.

(DeNale & Lukens, 1986)

DeNale, R. and Lukens, W. E. 1986. Increasing Contact Tube  
Life During Titanium Gas Metal Arc Welding. Welding  
Journal. 65:28-33

(Heald, 1990)

Heald, Paul 1990. Spray Metal Transfer in Gas Metal Arc  
Welding. T-3897. Master's thesis, Colorado School of  
Mines, Golden, Colo.

(Schey, 1983)

Schey, John A. 1983. Tribology in Metal Working; Friction, Lubrication and Wear. Metals Park, Ohio.: American Society for Metals.

(Siewert, 1991)

Interview with author. (303)-497-3000

(Yamada & Tanaka, 1987)

Yamada, T. and Tanaka, O. 1987. Fluctuation of the Wire Feed Rate in Gas Metal Arc Welding. Welding Journal. Sept:35-42.

#### FURTHER REFERENCES

Lancaster, 1984. The Physics of Welding. Ed. J.F. Lancaster, 1st ed. International Institute of Welding (IIW). Pergamon Press.

Shepard, M. E.; Cook, G,E,; Siewert T.A. 1987. Dynamic Modeling of Self-Regulation in Consumable Electrode Processes. in 68th American Welding Society Annual Meeting and 18th International AWS Brazing Conference. Chicago, Ill.

Samokovliisky, D.A. 1986. Wire Feed Systems for Robotic Mig Welding. Metal Construction (Bulgaria Academy of Sciences) V18: N5: 293-296.